

Polar Half-Metal and Triferroic Insulator based on PbMnO_3 : First-principles Theory

Arpita Paul¹ and *Umesh V. Waghmare*

Theoretical Sciences Unit

JNCASR, Bengaluru 560064 INDIA

¹Department of Physics, IIT Jammu



Funded by the Department of Science and Technology,
Government of India

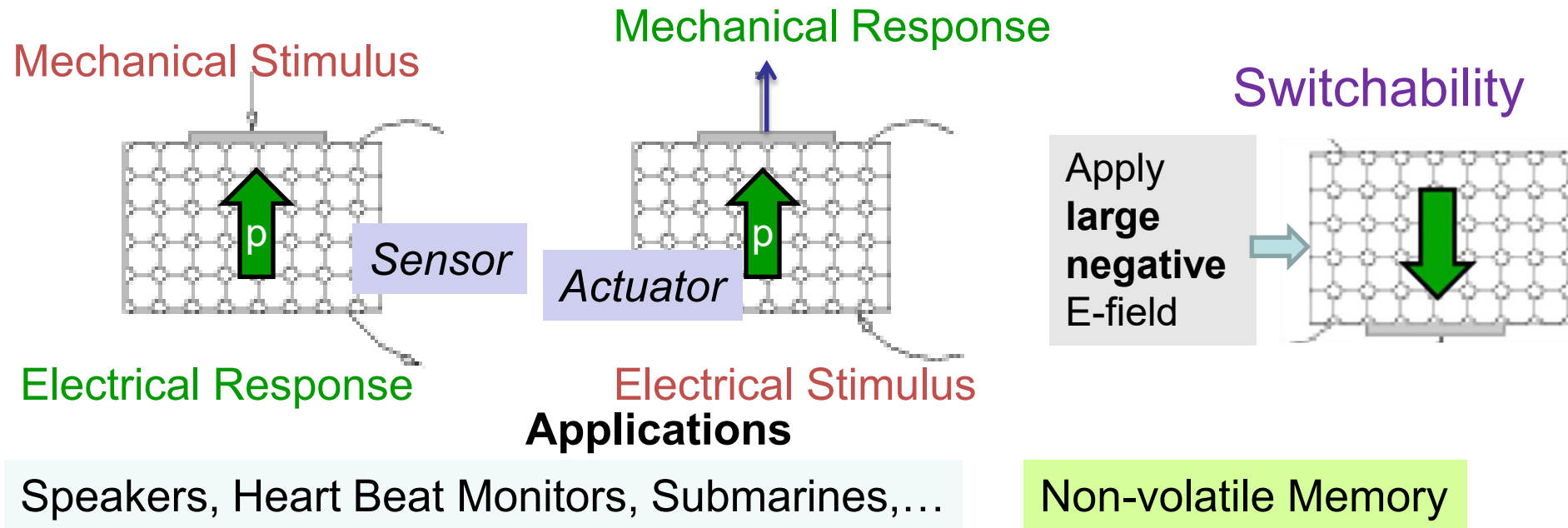
JC Bose National Fellowship

¹ *Inspire Faculty Fellowship*

March 2026
IIT Bombay

Polar Ferroic Materials: Ferroelectrics

Ferroelectrics: Smart Multifunctional Materials



Interesting Science of Materials,

- Properties tunable by Electric Field and Stress
- Extreme Sensitivity to boundary conditions (surrounding)

- M. E. Lines and A. M. Glass, Principles and Applications of Ferroelectrics and Related Materials, Oxford Univ Press (2001)
- MDawber, K M Rabe and J F Scott, Rev Mod Phys 77, 20183 (2005).

Emergence of Properties across a Ferroic Transition

BaTiO₃, PbTiO₃

Ferroelectric Transition

● Ba, Pb

● Ti

● O

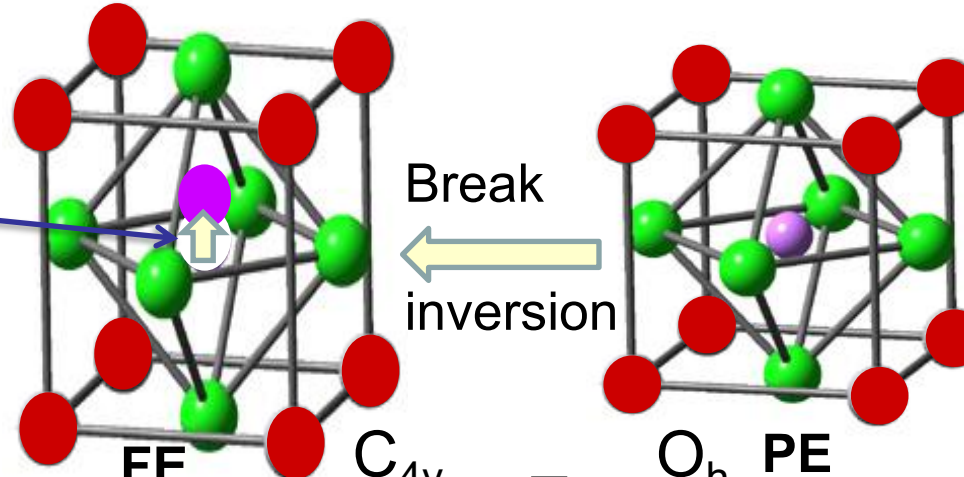
Electric Dipole p

Strain c/a

Break

inversion

Centrosymmetric



New Functional Properties ($T < T_o$):

Linear Piezoelectric



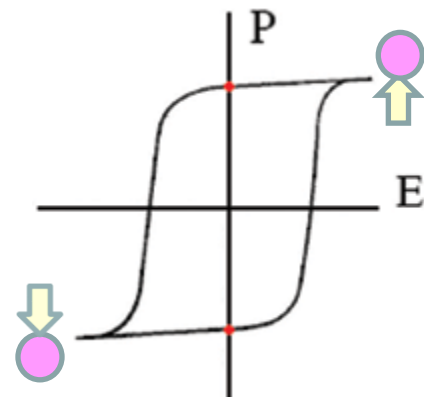
Sensors, Actuators, MEMS, Speakers

Nonlinear Hysteresis



Memory

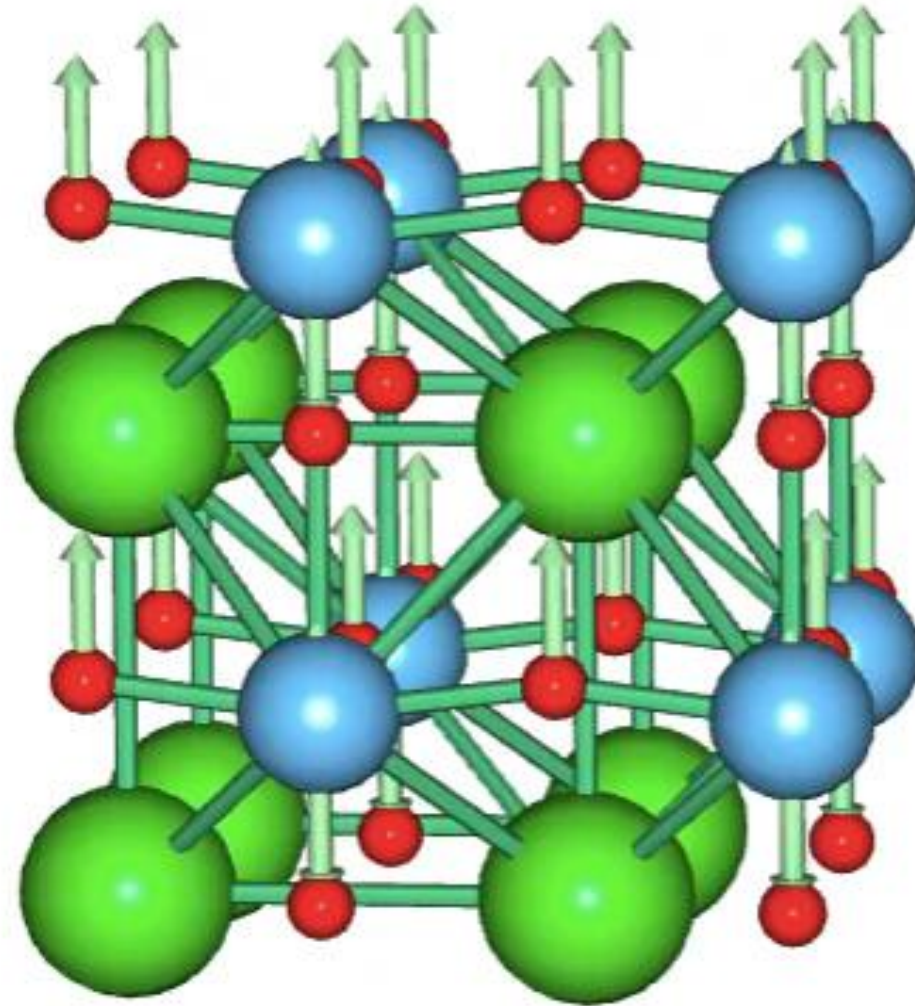
Applications



Near the Transition:

- Colossal piezo, dielectric properties
- Instability of Ti off-centering important!

TO Vibration (Phonon)
Associated with
**Ferroelectric Lattice
Instability:**
 BaTiO_3

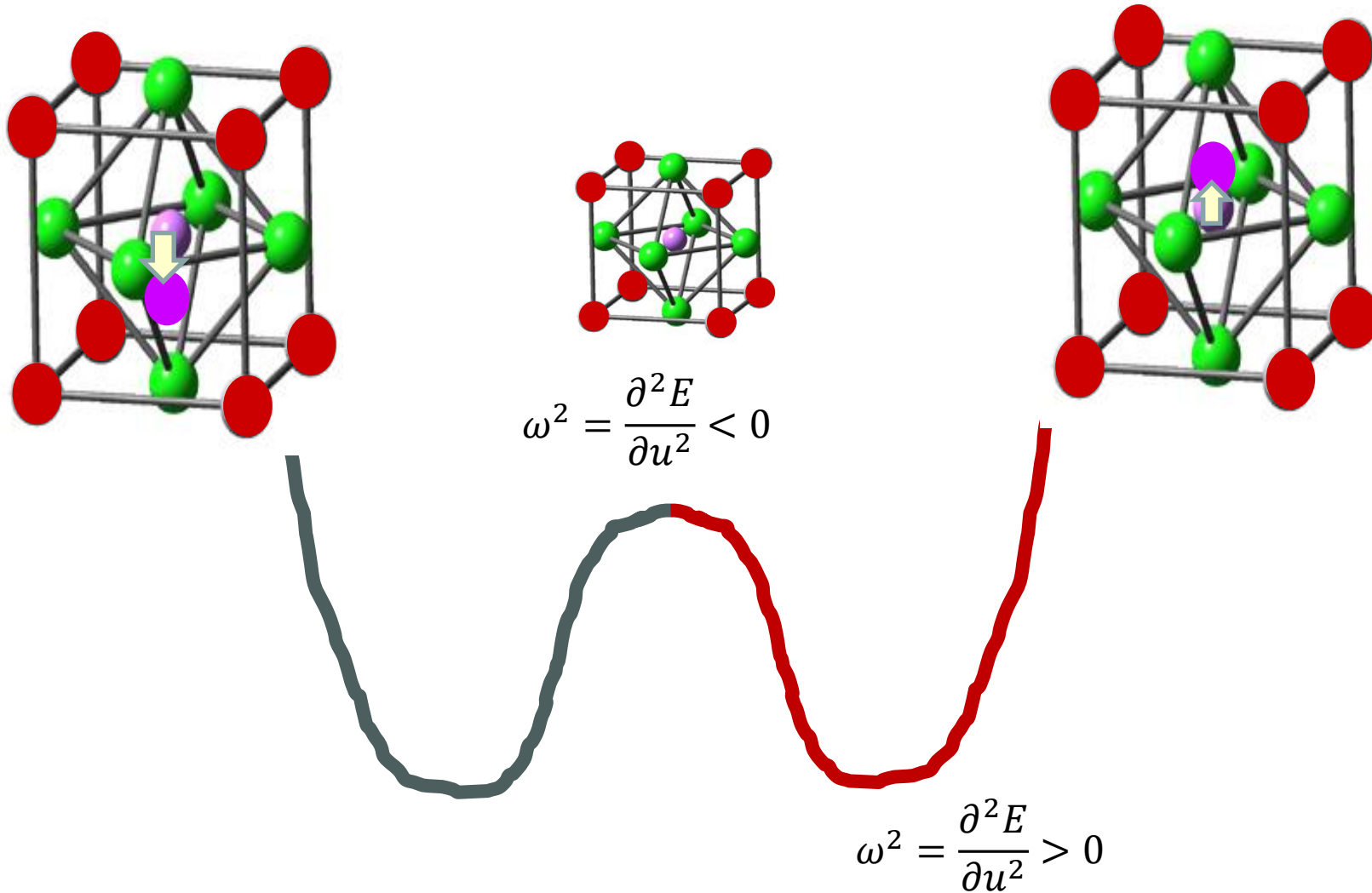


O

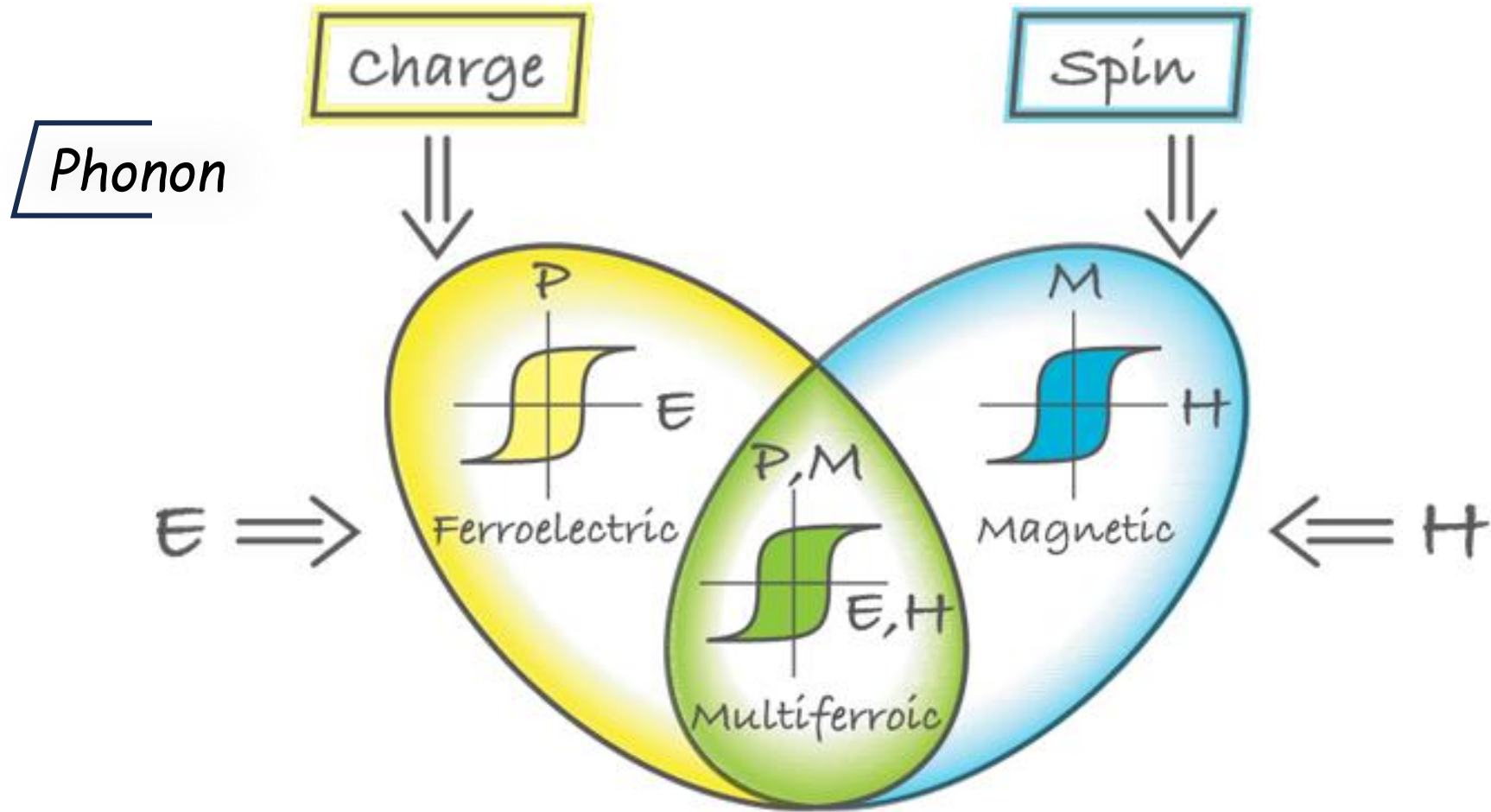
Ti

Ba

Lattice Instability



Interesting Science of Multi-ferroics



Transition Metal Oxides

ABO_3 perovskites

Symmetry Lowering Orders: Multi Ferroics

B

Ferroelectrics

$d^{n=0}$

Insulators

Polarity

BiFerroics

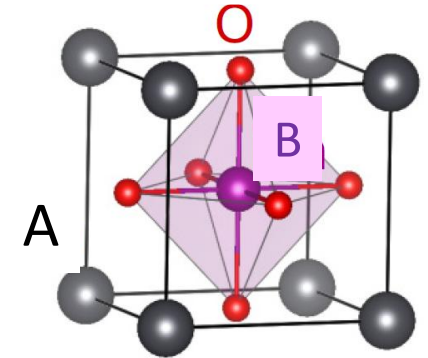
Half-metals

Ferromagnets

$d^{n \neq 0} \rightarrow S$

Metals

Inversion symmetry

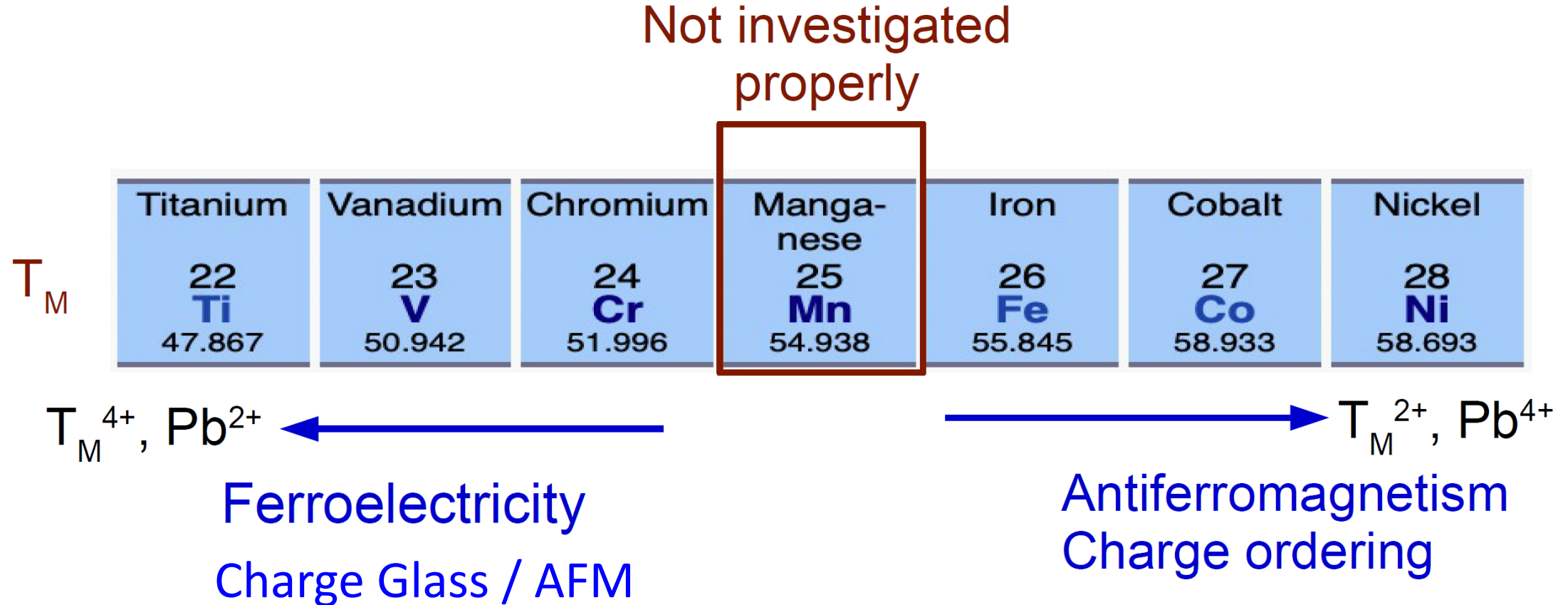


Polar Half-metallic Ferromagnet?

Puggioni et al, Phys Rev Mat 2, 114403 (2018)

- Metallic in one spin channel: Ferromagnet
- Gapped in the states of other spin channel: Polarization

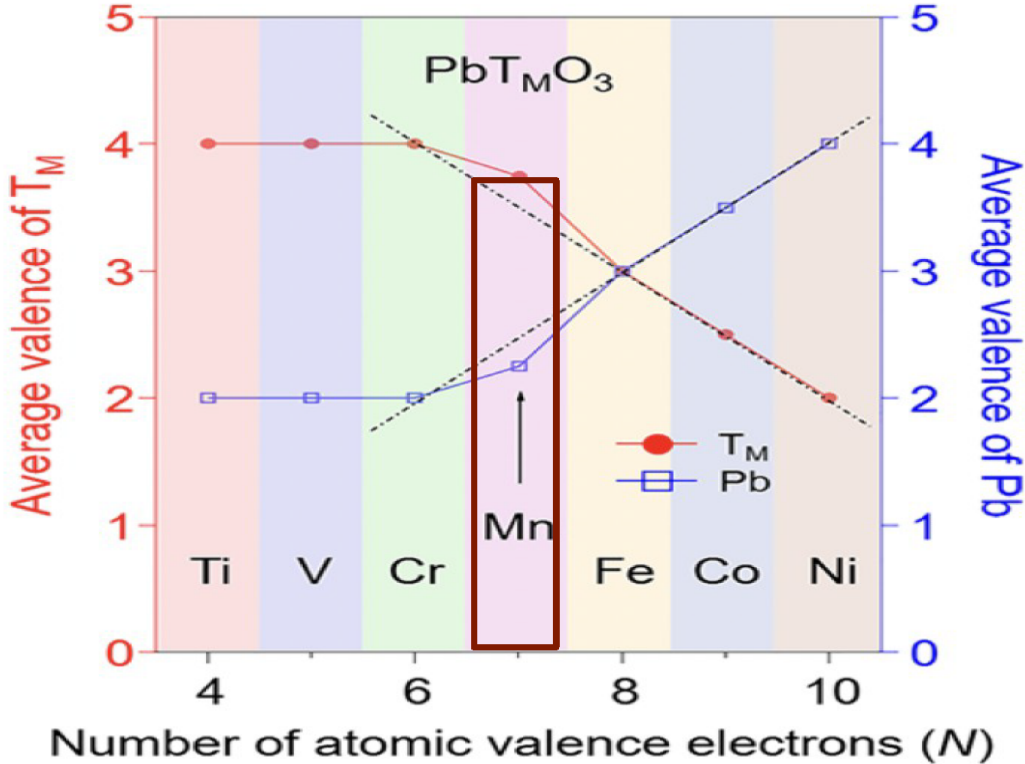
Valence State Crossover in $\text{Pb}T_M\text{O}_3$



Charge degree of freedom: Pb^{2+} ($6s^2$) and Pb^{4+} ($6s^0$)

Li et al, Chem Mater 33, 92 (2021)

Earlier studies on PbMnO_3



Goldschmidt tolerance factor

$$t = \frac{r_{Pb} + r_O}{\sqrt{2}(r_{T_M} + r_O)}$$

PbTiO_3 : $t=1.02$

PbMnO_3 : $t=1.01$

(structural distortion expected)

Li et. al., Chem. Mater 33, 92 (2021)

Nominal valence of Mn $\approx 4+$ (d^3)

Ambient pressure

Hexagonal perovskite (6H)
AFM insulator ($T_N=155$ K)

15 GPa

Perovskite (3C)

No consensus on

crystal structure

(polar/nonpolar),

electronic

(metal/insulator),

Magnetic (FM/AFM)

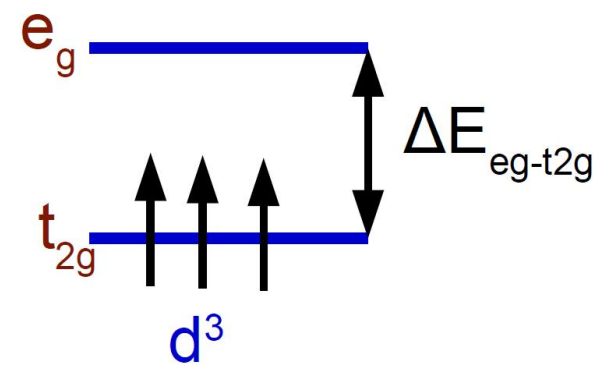
properties of 3C phase

Cubic SrMnO_3 and PbMnO_3

Lattice parameter:
 $a(\text{SrMnO}_3) < a(\text{PbMnO}_3)$

PbMnO_3 : Small $\Delta E_{eg-t_{2g}}$

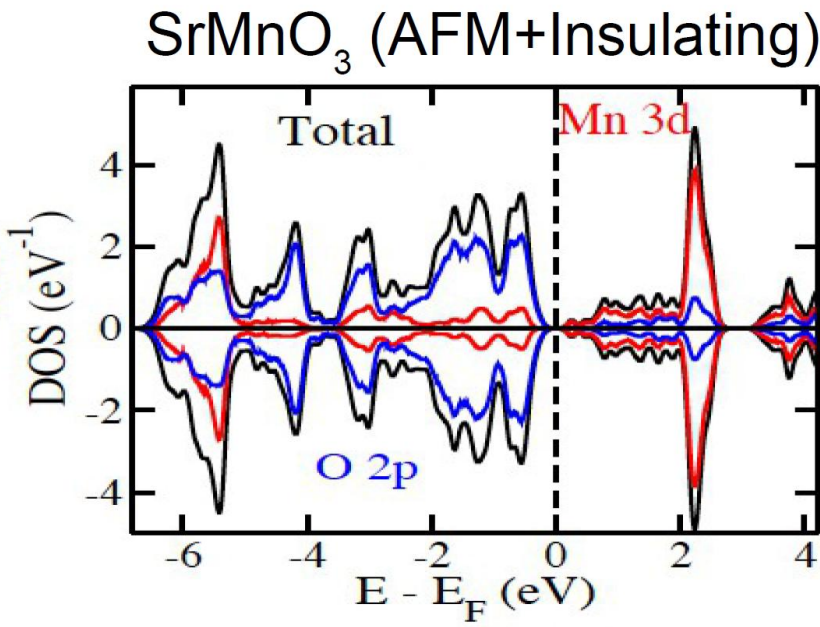
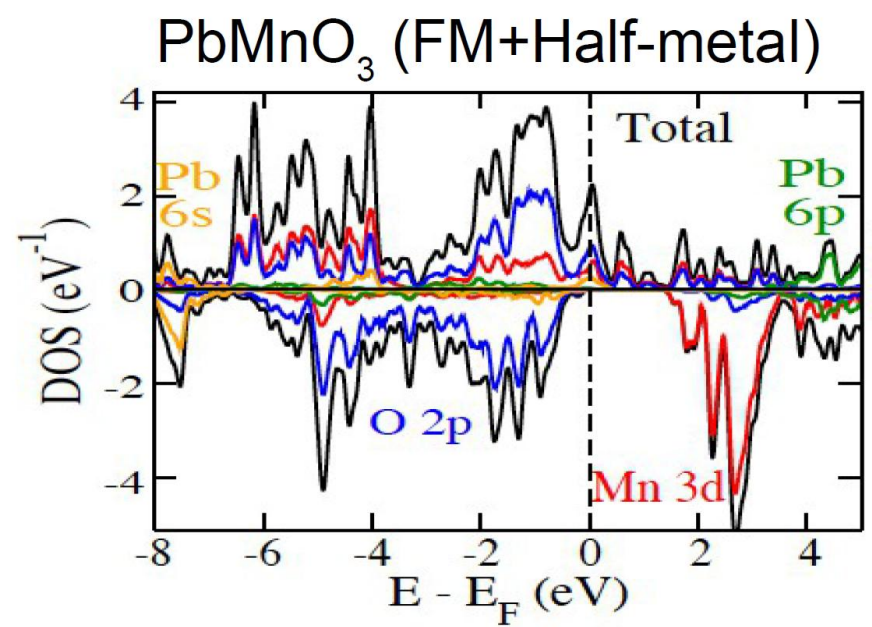
e_g-t_{2g} hopping increases
(FM interaction)



d^3 perovskite
(Half-filled)

SrMnO_3 : G-AFM

PbMnO_3 : FM



Instabilities of the Cubic ($Pm\bar{3}m$) structure of $PbMnO_3$ and $SrMnO_3$

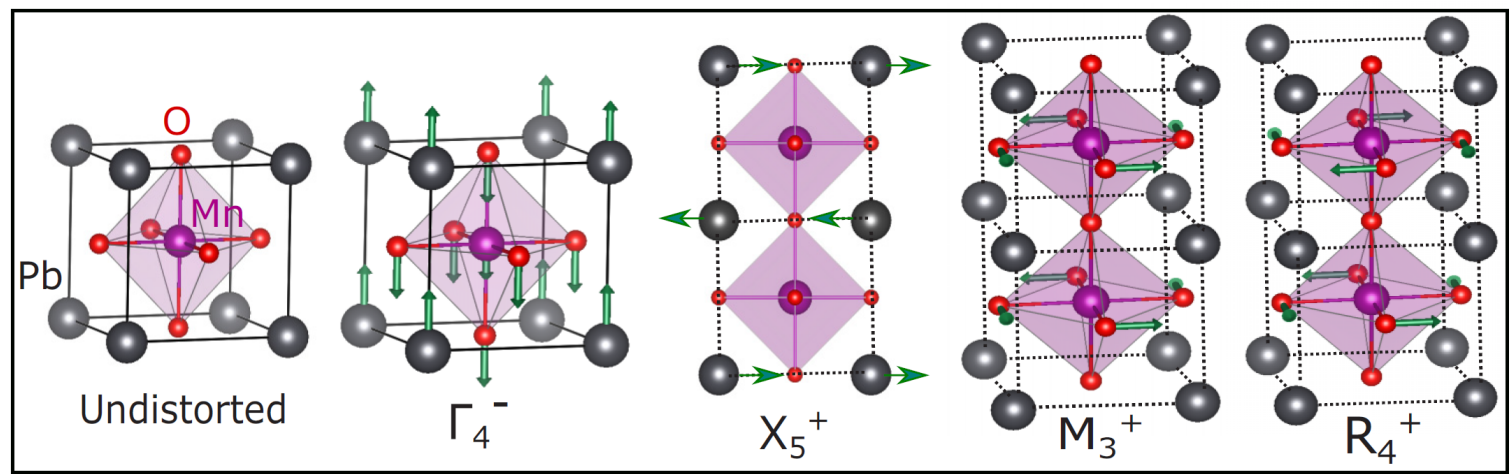
TABLE II. Our calculated phonon frequencies (in cm^{-1}) of polar (Γ_4^-), antipolar (X_5^+), and nonpolar (M_3^+ and R_4^+) phonon modes of cubic ($Pm\bar{3}m$) $PbMnO_3$ and $SrMnO_3$ in FM and G-AFM states, in comparison with earlier results [38]. Phonon frequencies of G-AFM $PbMnO_3$ (FM $SrMnO_3$) at the optimized lattice constant of cubic FM (G-AFM) structure are also computed.

| Phase | Γ_4^- (cm^{-1}) | X_5^+ (cm^{-1}) | M_3^+ (cm^{-1}) | R_4^+ (cm^{-1}) |
|---|-----------------------------------|------------------------------|------------------------------|------------------------------|
| | $PbMnO_3$ | | | |
| FM ($a = 3.84 \text{ \AA}$) | $i45$ | 28 | $i163$ | $i180$ |
| G-AFM ($a = 3.84 \text{ \AA}$) | $i64$ | 43 | $i104$ | $i122$ |
| G-AFM ($a = 3.82 \text{ \AA}$) | $i13$ | 51 | $i93$ | $i117$ |
| | $SrMnO_3$ | | | |
| FM ($a = 3.78 \text{ \AA}$) | $i90$ | 124 | $i110$ | $i136$ |
| G-AFM ($a = 3.78 \text{ \AA}$) | 164 | 123 | 51 | $i88$ |
| G-AFM ($a = 3.80 \text{ \AA}$, HSE [38]) | 177 [38] | — | — | 64 [38] |
| G-AFM ($a = 3.80 \text{ \AA}$, $U = 2.8 \text{ eV}$ [38]) | 217 [38] | — | — | $i71$ [38] |

Contrast: PMO is unstable; G-AFM SMO is weakly unstable

Lattice Instabilities

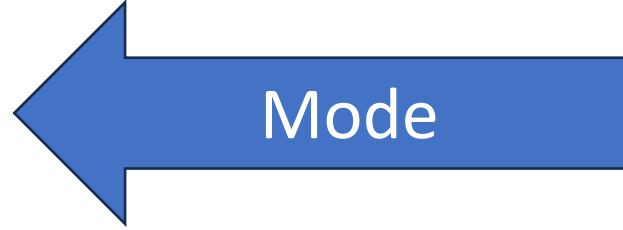
Of Cubic PbMnO_3



Polar Antipolar Antiferrodistortive

Structural Distortions of Cubic PbMnO_3

Low Symmetry
structure

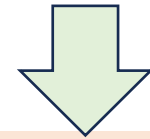


Mode

$Pm\bar{3}m$ (*cubic high symm*)

TABLE III. Energetics of polar and nonpolar phases of PbMnO_3 with FM and G-AFM orderings. The structural distortion is given with respect to the undistorted cubic structure ($Pm\bar{3}m$ symmetry group). $\Delta E = E_{\text{G-AFM}} - E_{\text{FM}}$, is the energy difference between FM and G-AFM states.

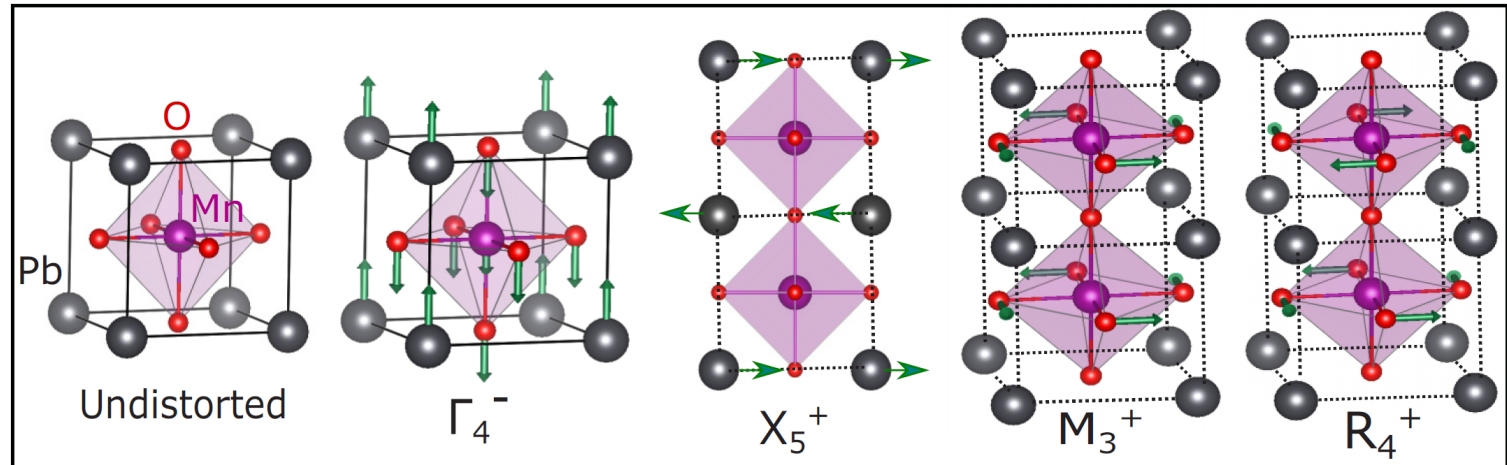
| Phase | Rotation pattern | Distortion | Phase | E_{FM} (meV/f.u.) | ΔE (meV/f.u.) |
|--------------|------------------|---|----------|----------------------------|-----------------------|
| $Pm\bar{3}m$ | $a^0 a^0 a^0$ | undistorted | Nonpolar | 146 | 88 |
| $P4mm$ | $a^0 a^0 a^0$ | $\Gamma_4^- [001]$ | Polar | 139 | 95 |
| $Amm2$ | $a^0 a^0 a^0$ | $\Gamma_4^- [110]$ | Polar | 142 | 93 |
| $I4/mcm$ | $a^0 a^0 c^-$ | $R_4^+ [001]$ | Nonpolar | 35 | 180 |
| $R\bar{3}c$ | $a^- a^- a^-$ | $R_4^+ [111]$ | Nonpolar | 10 | 207 |
| $Imma$ | $a^- a^- c^0$ | $R_4^+ [110]$ | Nonpolar | 12 | 200 |
| $Pnma$ | $a^- a^- c^+$ | $R_4^+ [110] + M_3^+ [001] + X_5^+ [110]$ | Nonpolar | 0 | 209 |



PbMnO_3 : *FM state* remains lower in energy than the AFM
Pnma is the lowest energy structure

Lattice Instabilities

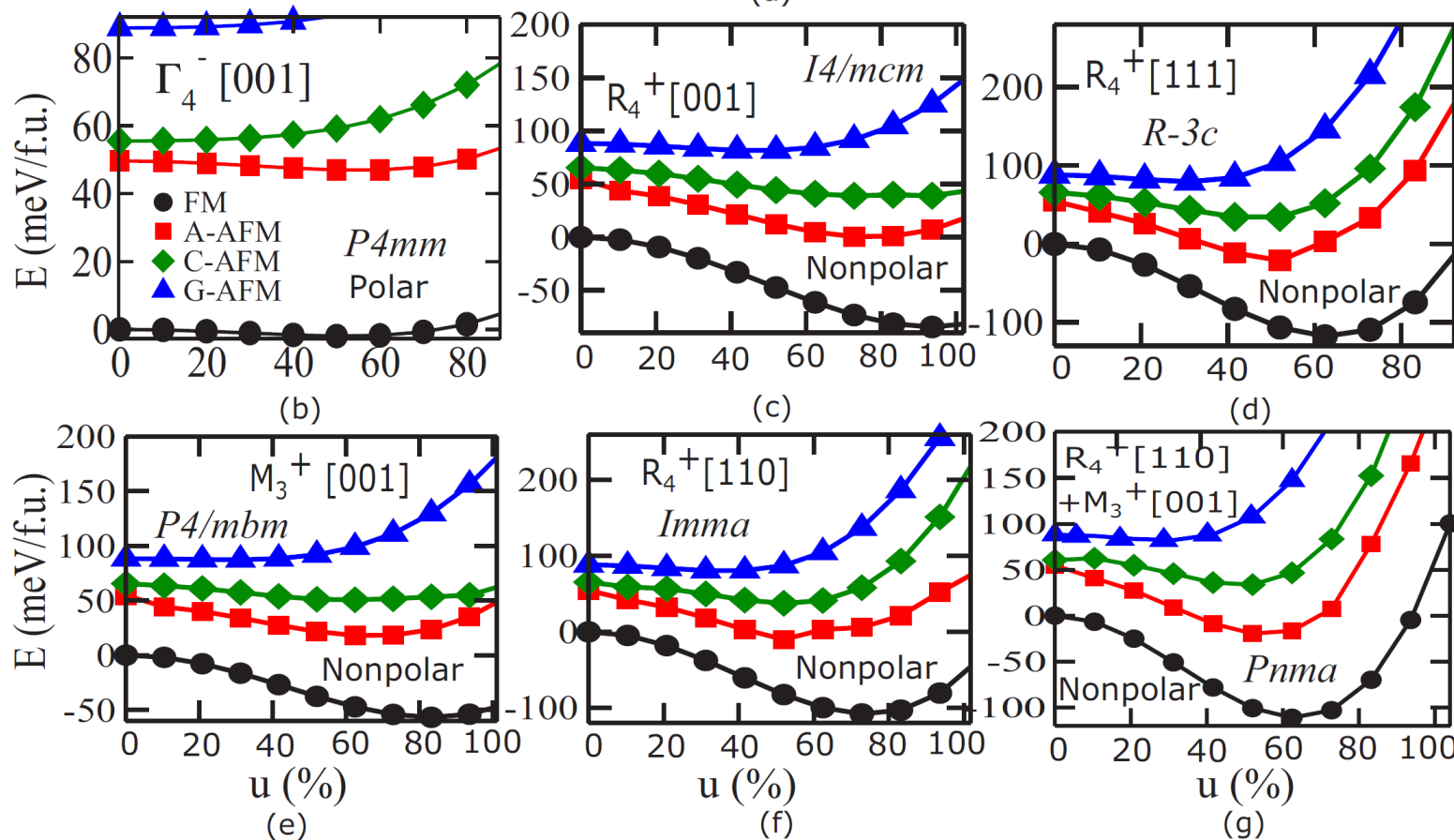
Of Cubic PbMnO_3



(a)

Strong Instabilities of MnO_6 octahedral Rotations

FE instability is weak



(b)

(c)

(d)

(e)

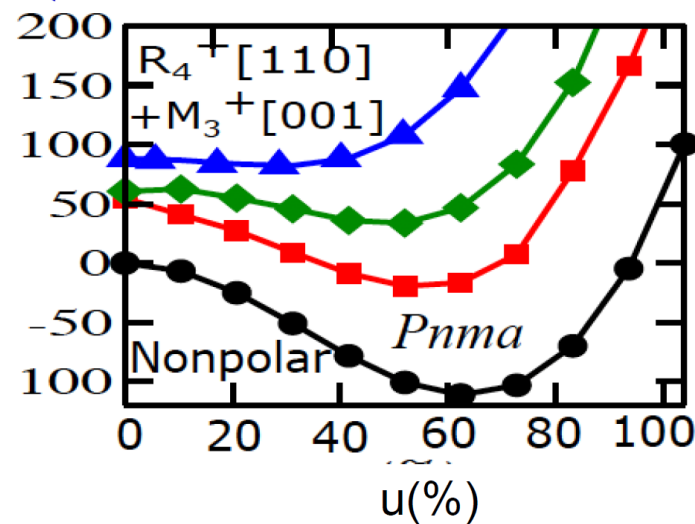
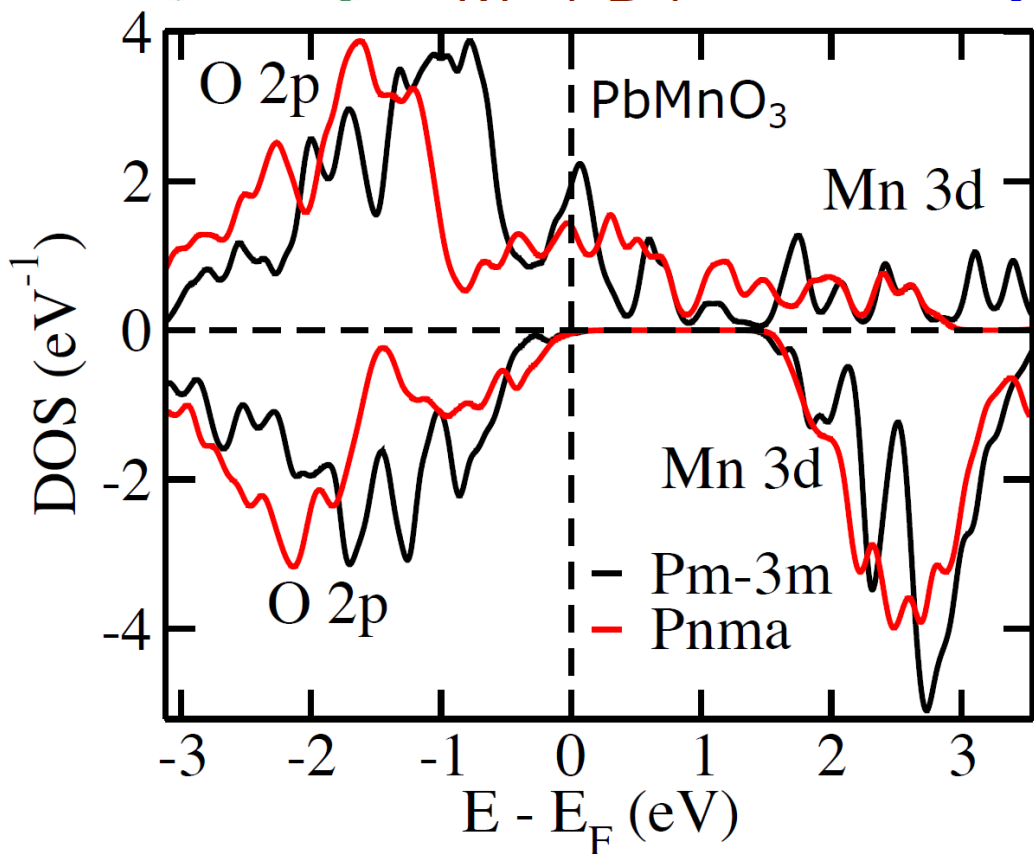
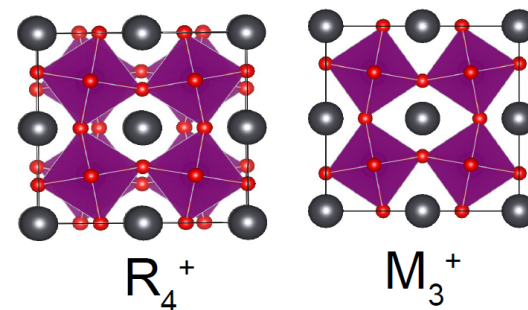
(f)

(g)

Crystal & Electronic Structure of PbMnO_3

| | | | |
|-------------------------------|--------------|---------|---------|
| ω (cm^{-1}) | Γ_4^- | M_3^+ | R_4^+ |
| FM | i45 | i163 | i180 |

Strong antiferro-distortive/rotational instabilities



Lowest energy structure: Nonpolar $Pnma$ phase ($a^-a^+c^+$)
FM Half-metal

2nd order phonon-spin coupling

How to make PbMnO_3 multiferroic?

Engineering polar phases in PbMnO_3

Mn^{4+} : d^3
(Half-filled)

Cubic PbMnO_3

Ferromagnetic
Half-metal

Unstable modes: R_4^+ and M_3^+
Rotation of MnO_6 octahedra

Unstable polar phonon
mode: Γ_4^-

Competition

Nonpolar orthorhombic
phase

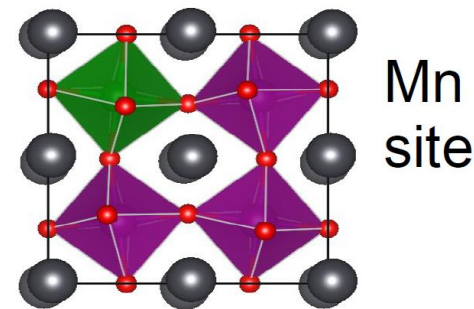
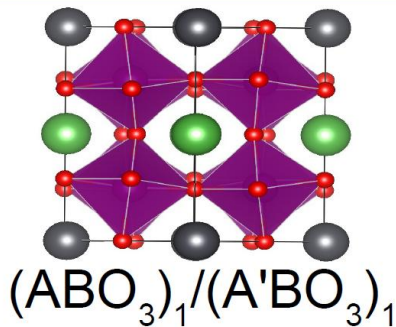
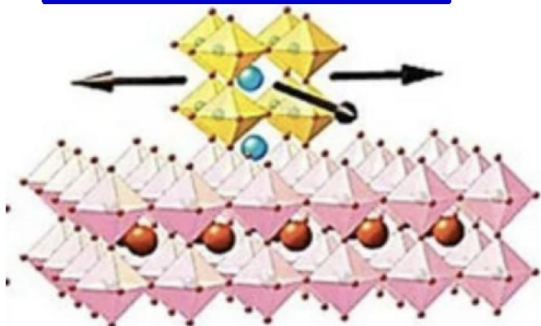
Ferromagnetic
Half-metal

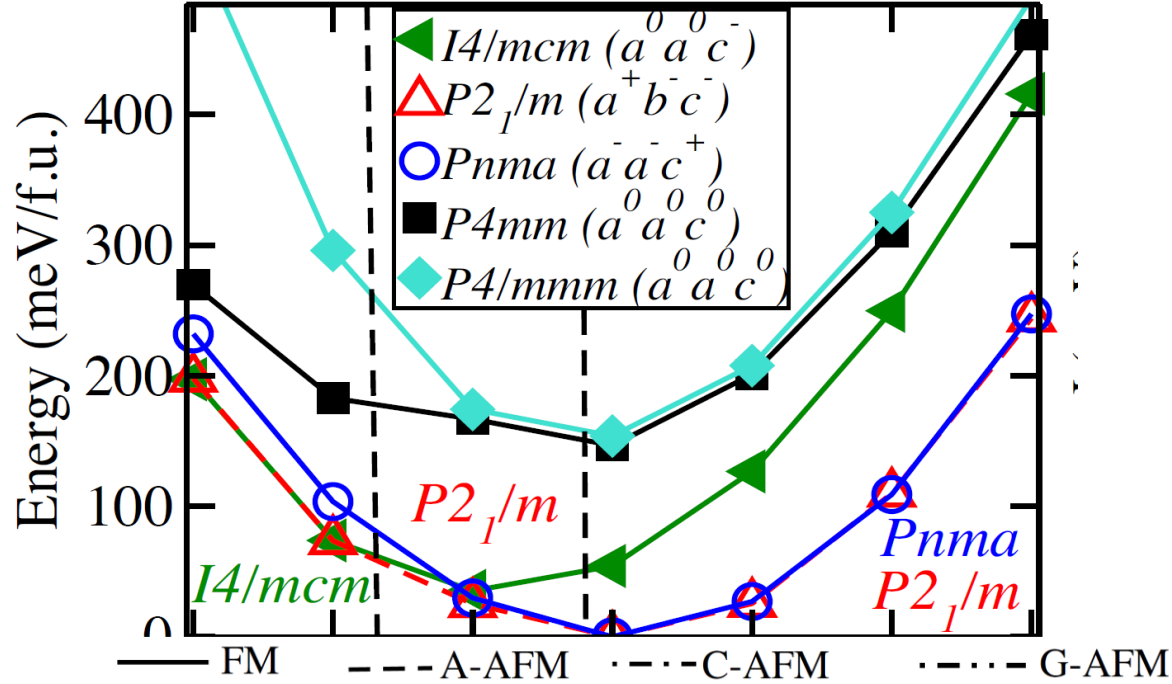
Stabilizing polar phases

X
Epitaxial strain

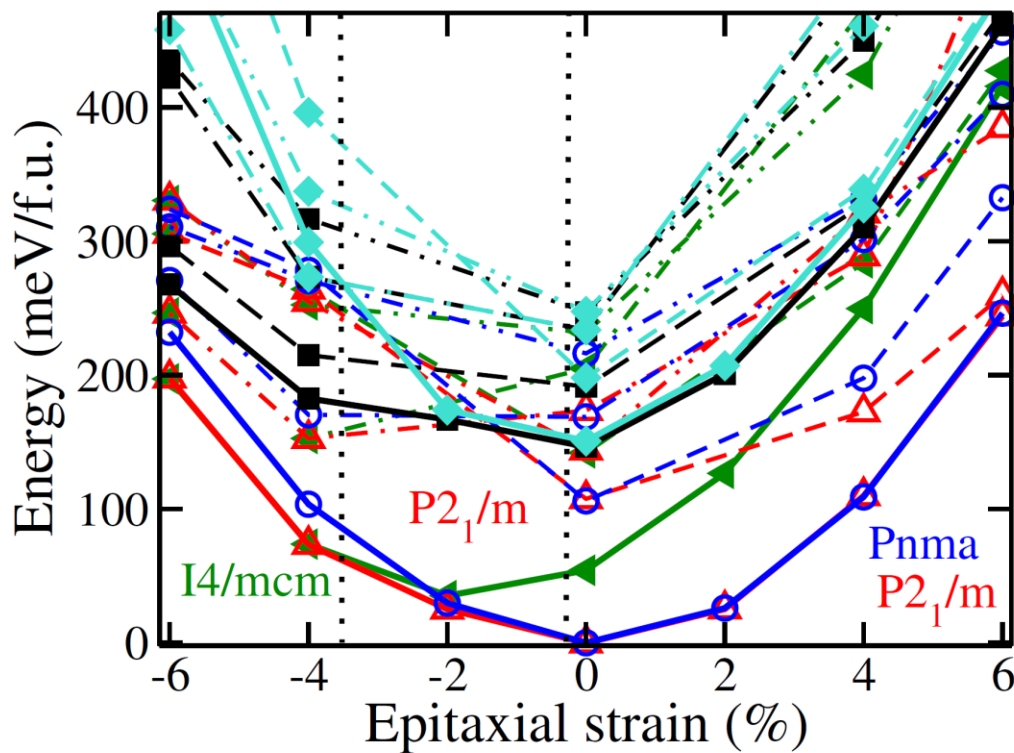
✓
Hetero-structuring

X
Cation substitution





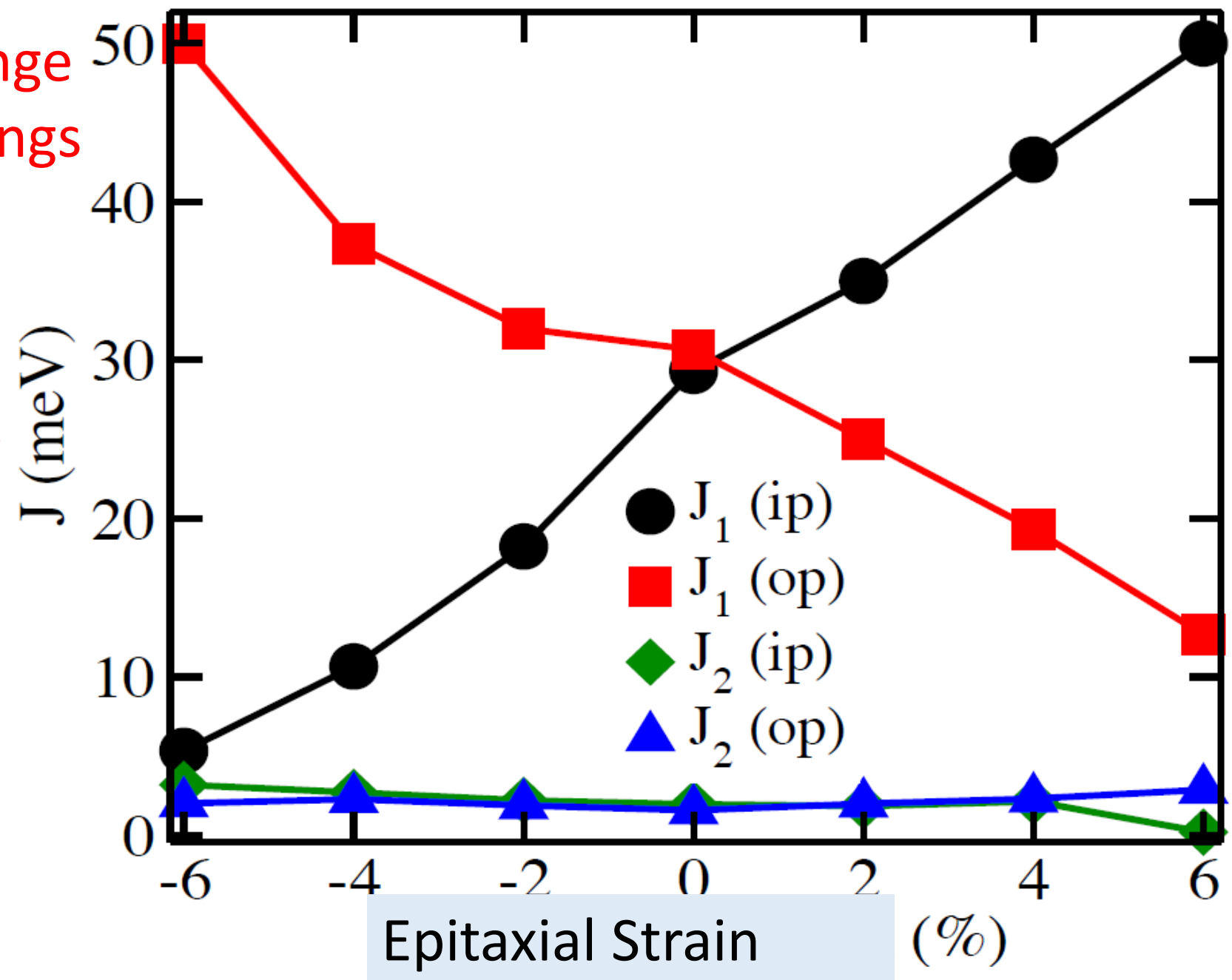
Can Epitaxial Strain
Make $PbMnO_3$ *Polar*?



A-AFM: (001)
 C-AFM: (110)
 G-AFM: (111)
 FM: (000)

No! Nonpolar HMFM is robust

Exchange Couplings



PbMnO₃:
Strong
Magneto
Striction!

Can Substitution at B-site make PbMnO_3 *Polar*?

TABLE S2: Our estimates of phonon frequencies (in cm^{-1}) of polar (Γ_4^-) and nonpolar antiferrodistortive (M_3^+ and R_4^+) phonon modes of ferromagnetic $\text{PbMn}_{0.875}\text{TM}_{0.125}\text{O}_3$ ($\text{TM}=\text{Ti}$ and Nb) in the $Pm\bar{3}m$ structure (undistorted phase).

| Compound | Γ_4^- (cm^{-1}) | M_3^+ (cm^{-1}) | R_4^+ (cm^{-1}) |
|--|-----------------------------------|------------------------------|------------------------------|
| PbMnO_3 | <i>i</i> 45 | <i>i</i> 163 | <i>i</i> 180 |
| $\text{PbMn}_{0.875}\text{Nb}_{0.125}\text{O}_3$ | <i>i</i> 46 | <i>i</i> 128 | <i>i</i> 147 |
| $\text{PbMn}_{0.875}\text{Ti}_{0.125}\text{O}_3$ | <i>i</i> 50 | <i>i</i> 145 | <i>i</i> 168 |

Ti & Nb: Strengthen polar,
weaken T_MO_6 rotational instabilities

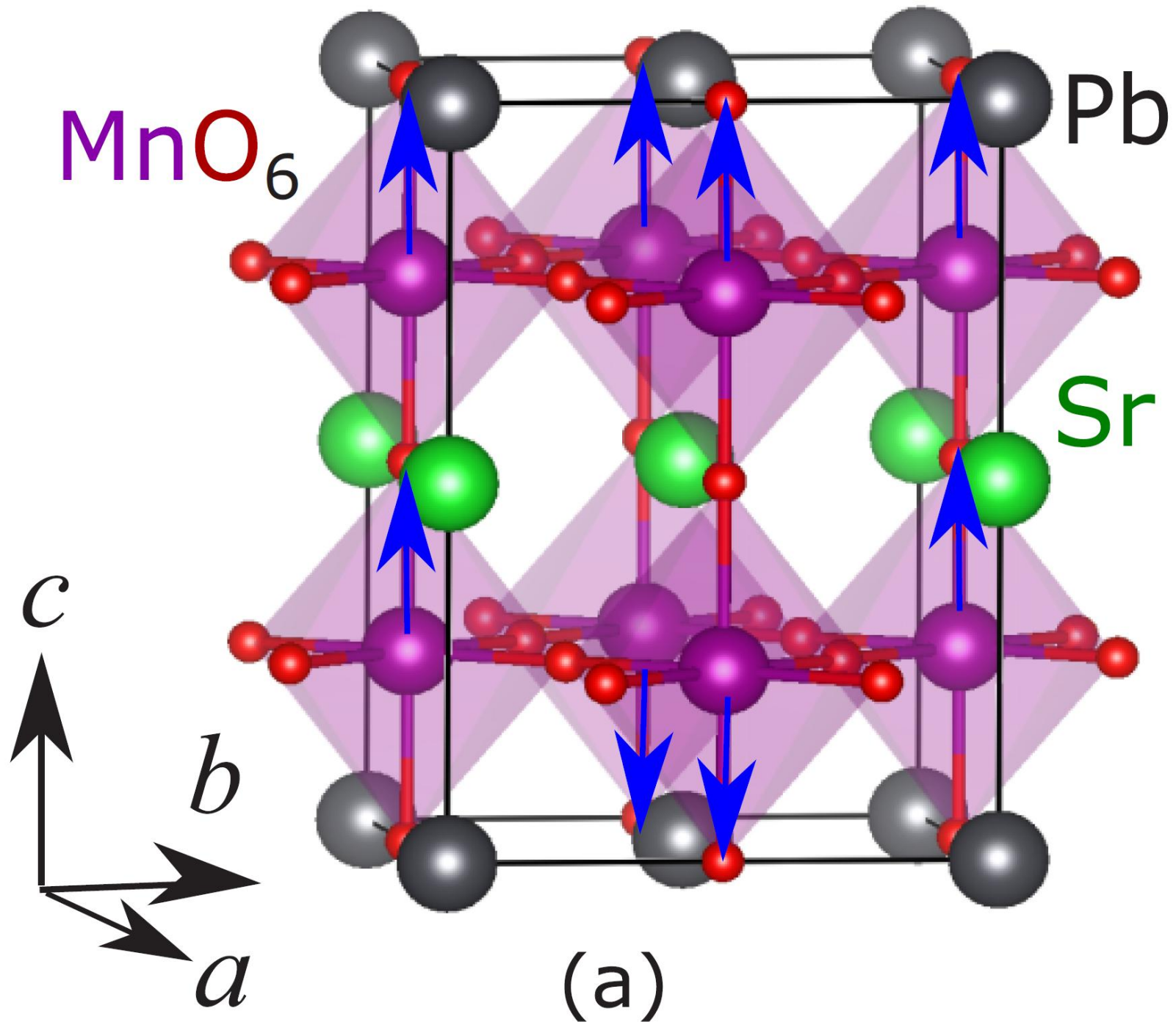
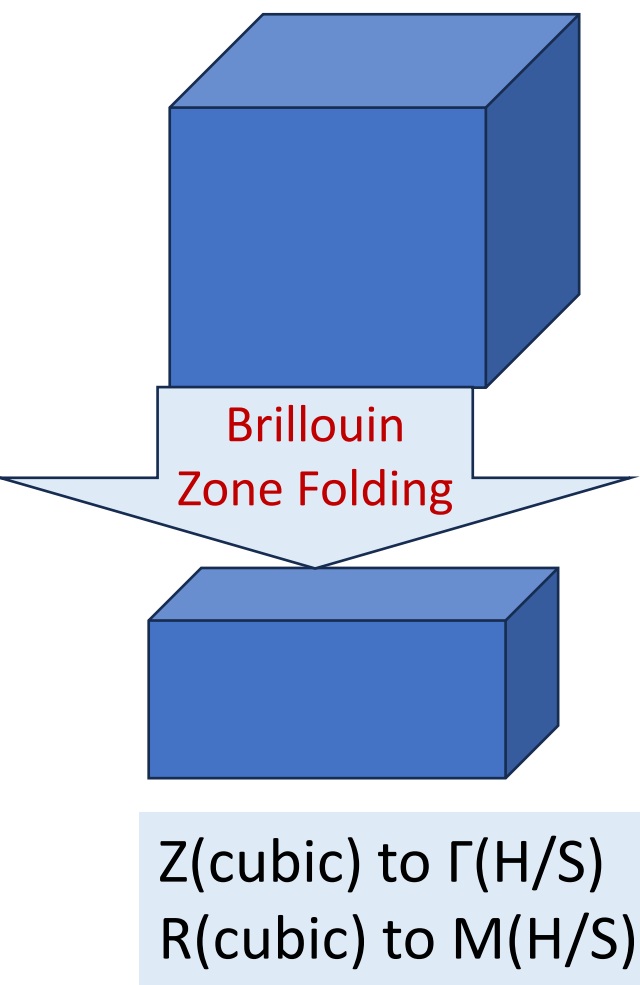
Can Substitution at B-site
make PbMnO_3 *Polar*?

No!

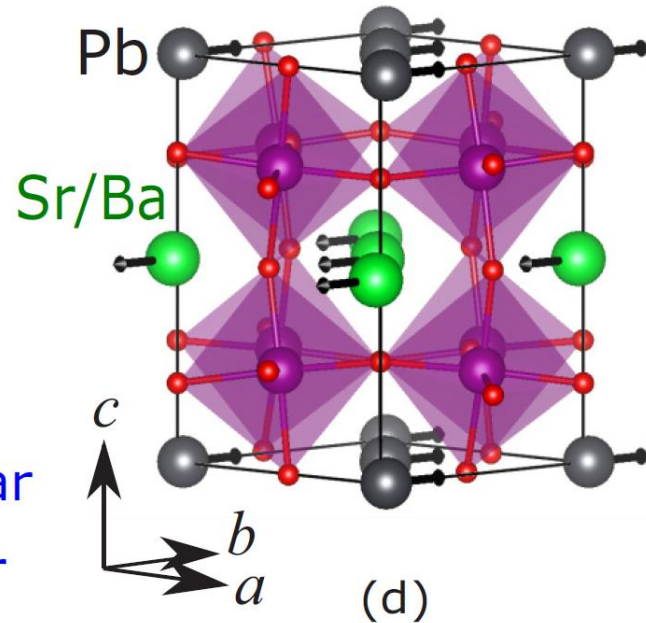
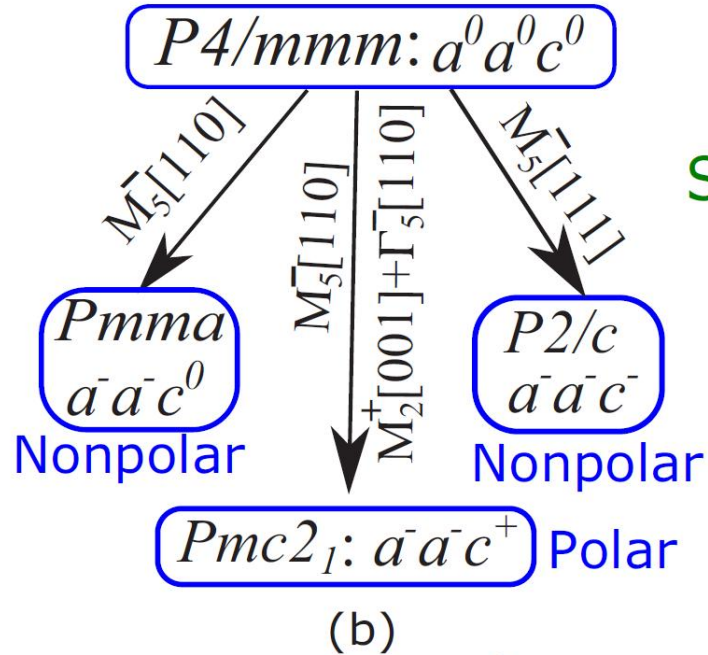
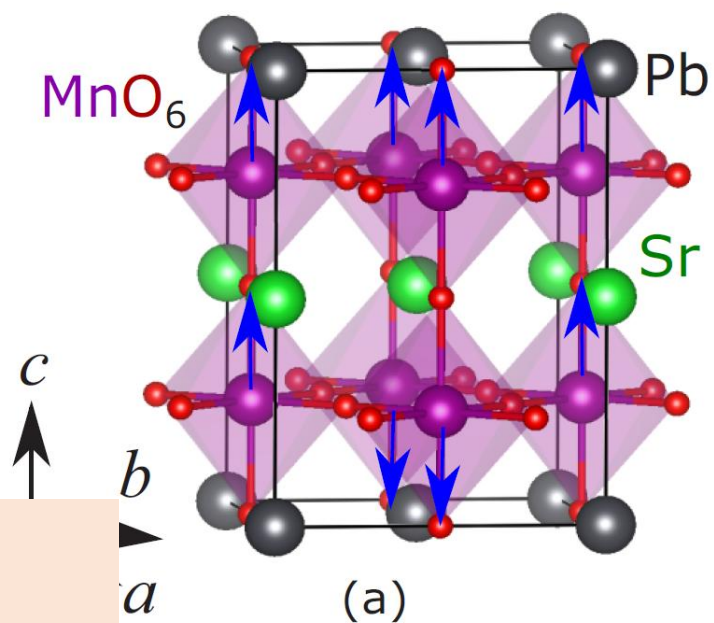
TABLE S1: Structural distortion (Δ_d), bond angle Mn-O-Mn, energy difference between FM and G-AFM states, and unit cell ($2 \times 2 \times 2$ supercell of five atomic perovskite unit cell) volume of $\text{PbMn}_{0.875}M_{0.125}\text{O}_3$ ($M=\text{V}$, Ti and Nb) with ferromagnetic ordering.

| Compound | Mn-O-Mn ($^\circ$) | Δ_d (10^{-5}) | $E_{G-AFM} - E_{FM}$ (meV/f.u.) | V (\AA^3) |
|--|----------------------|--------------------------|---------------------------------|------------------------|
| PbMnO_3 | 159 | 0.2 | 209 | 461 |
| $\text{PbMn}_{0.875}\text{V}_{0.125}\text{O}_3$ | 161 | 0.3 (away from V) | 127 | 461 |
| | 168 (V-O-Mn) | 9.0 | | |
| $\text{PbMn}_{0.875}\text{Nb}_{0.125}\text{O}_3$ | 162 | 8.1 | 132 | 468 |
| | 172 (Nb-O-Mn) | 0.5 (away from Nb) | | |
| $\text{PbMn}_{0.875}\text{Ti}_{0.125}\text{O}_3$ | 161 | 7.8 | 129 | 462 |
| | 167 (Ti-O-Mn) | 0.2 (away from Ti) | | |

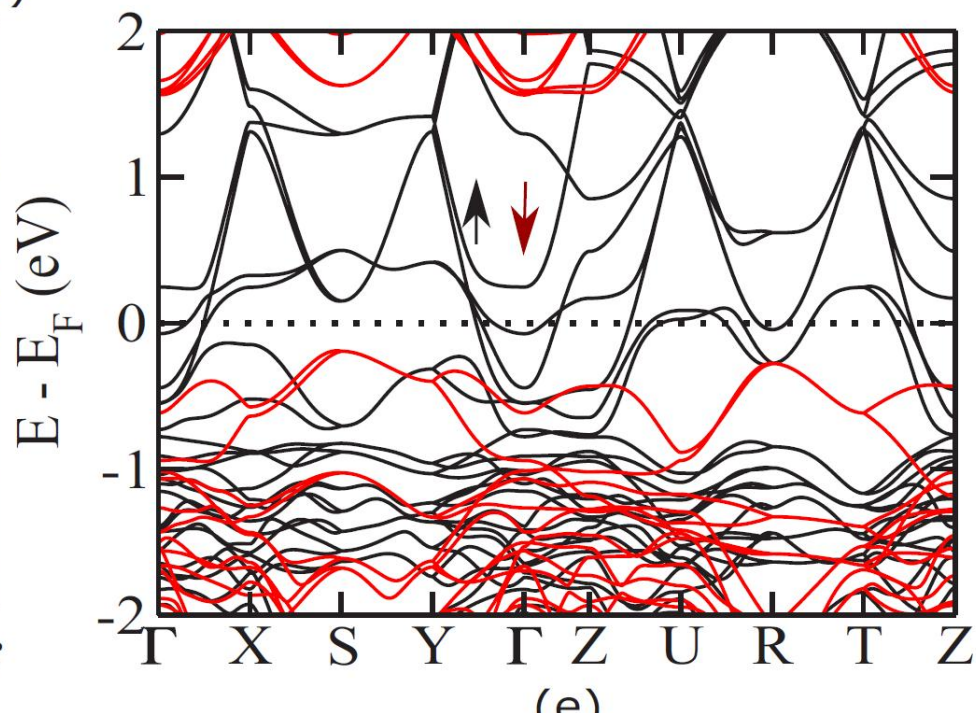
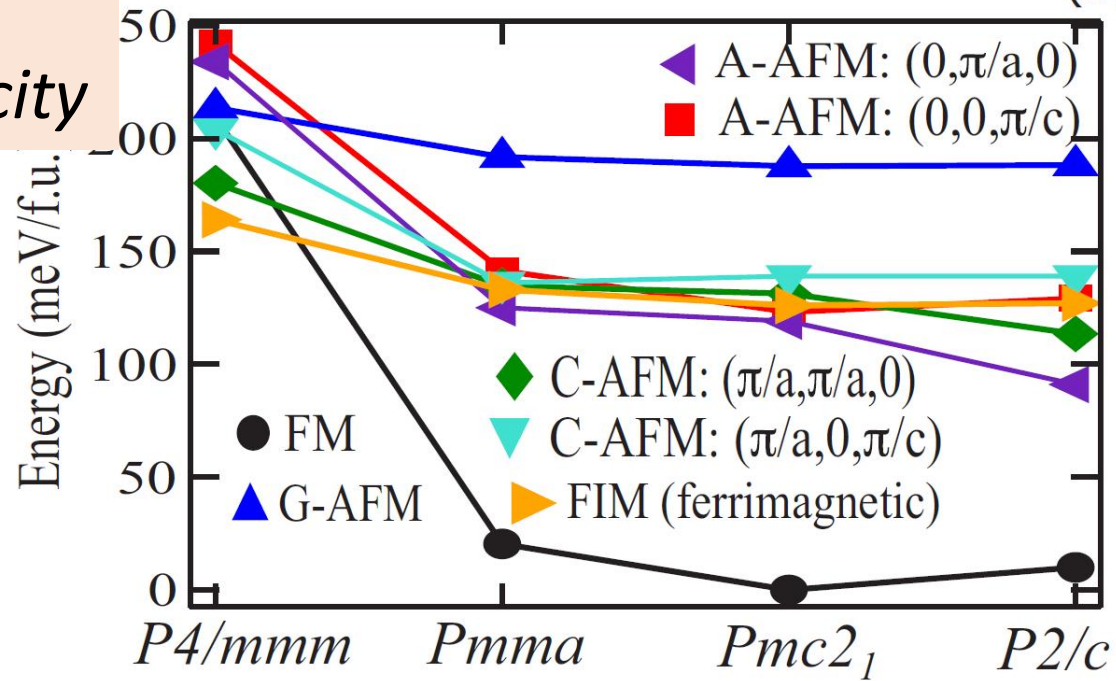
Heterostructure PbMnO_3 : SrMnO_3

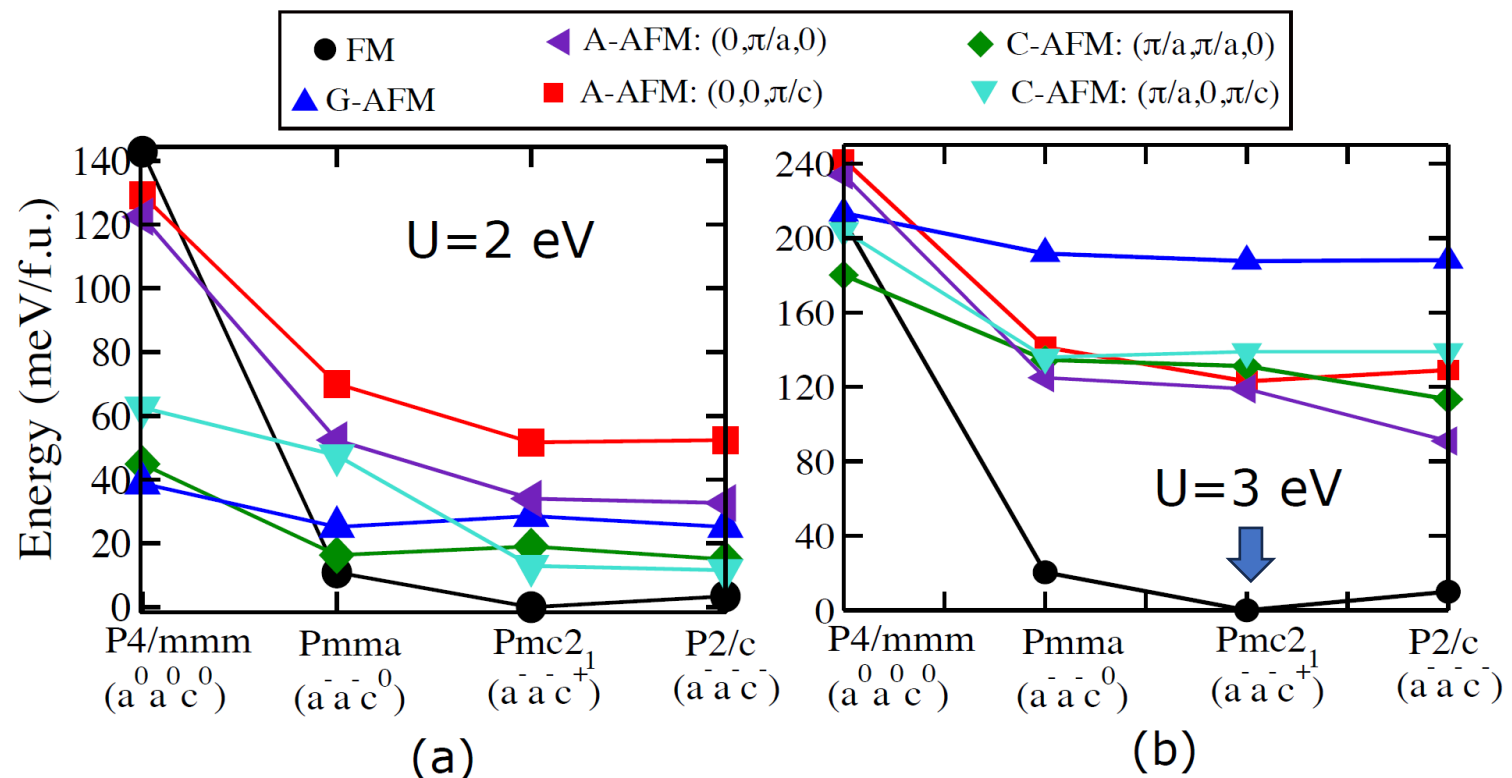


Heterostructure: PbMnO_3 : SrMnO_3

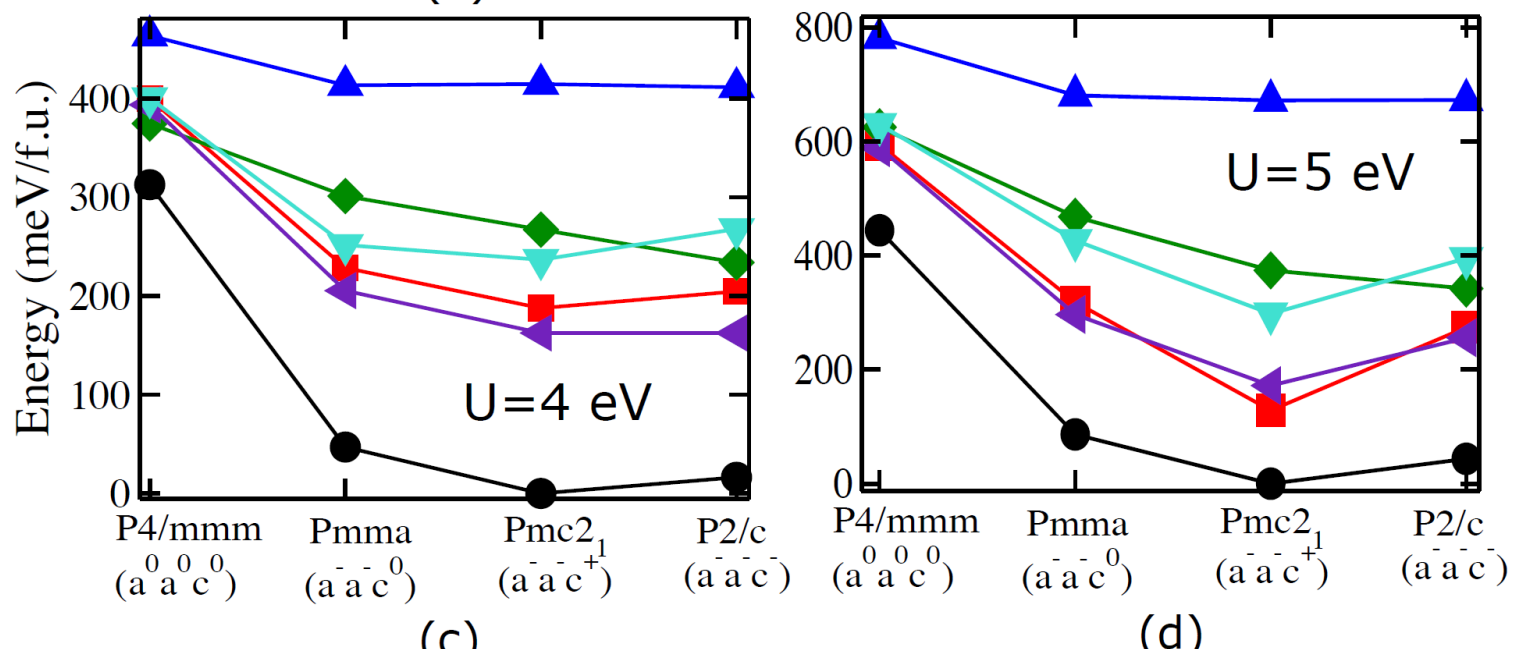


Hybrid
Improper
Ferroelectricity





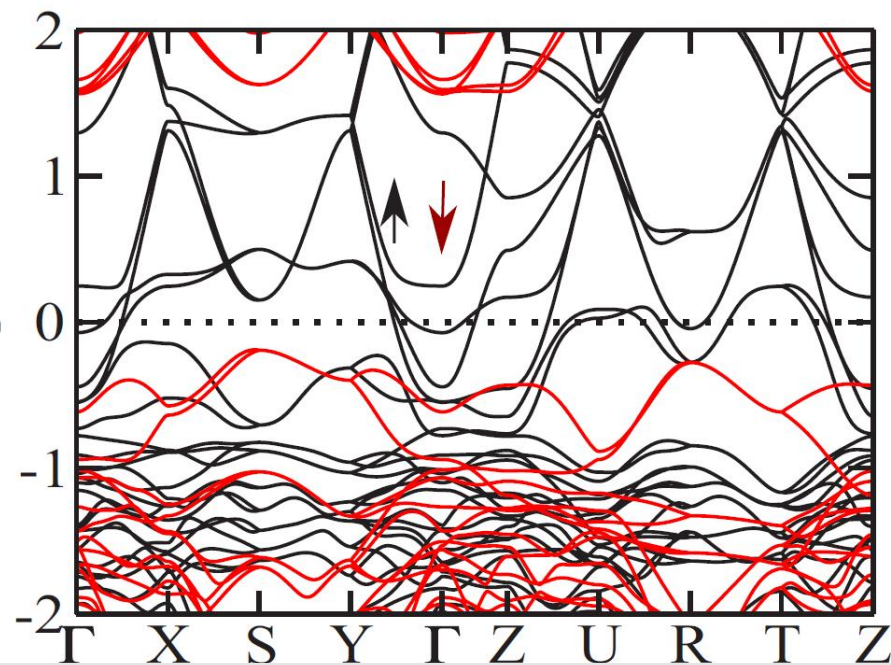
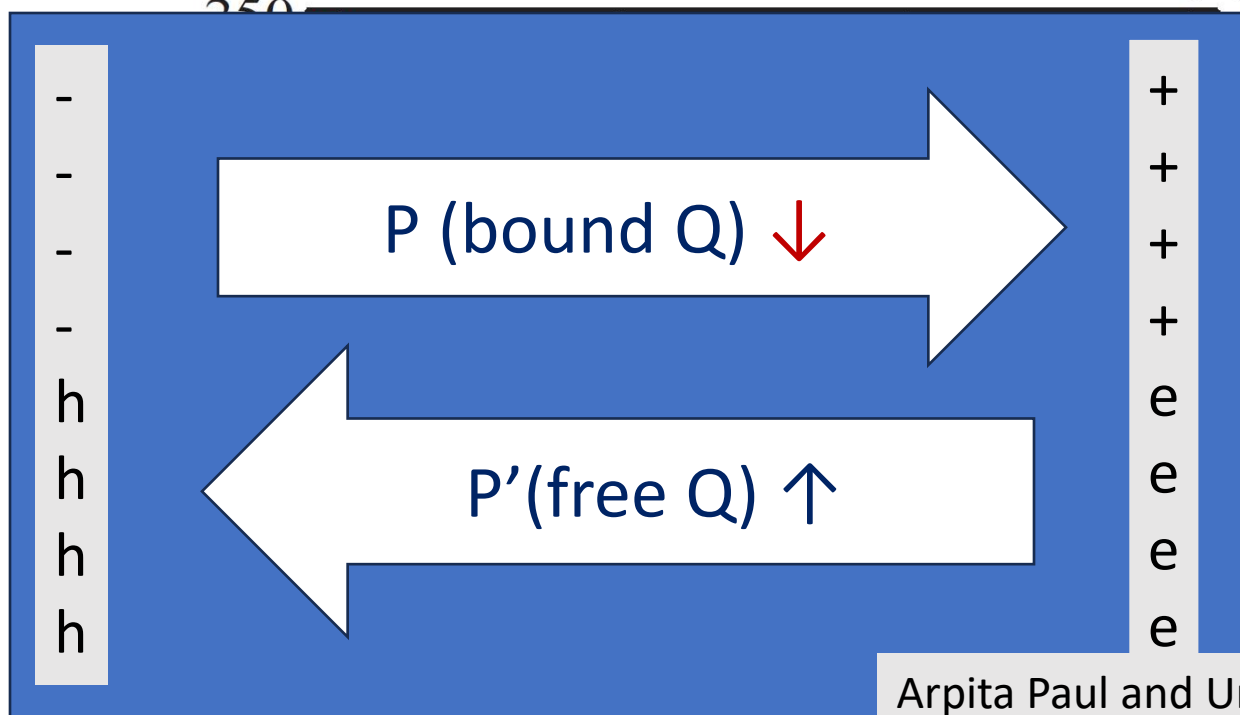
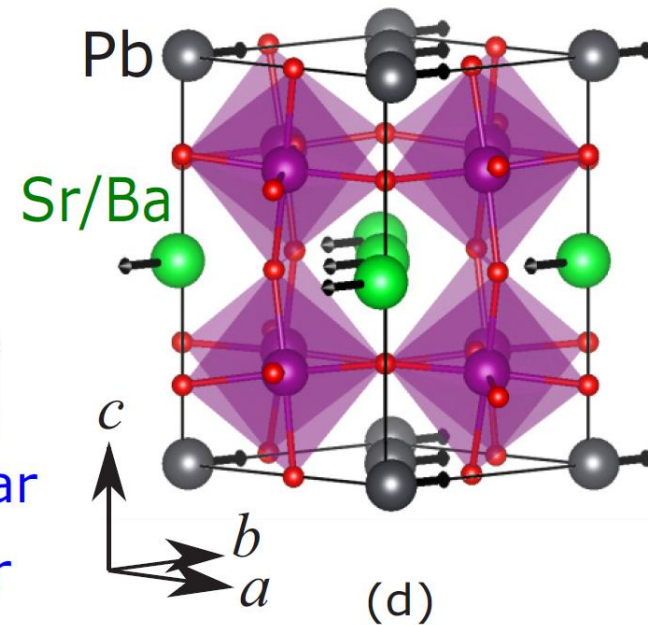
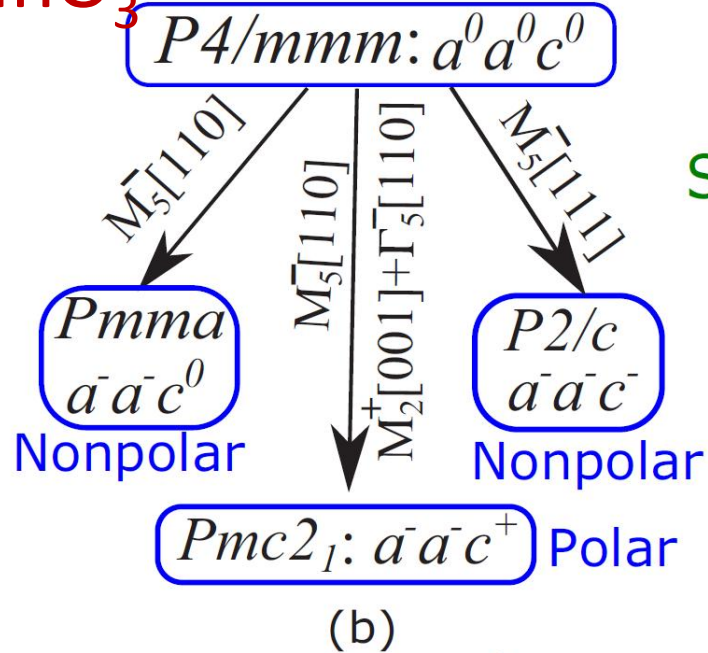
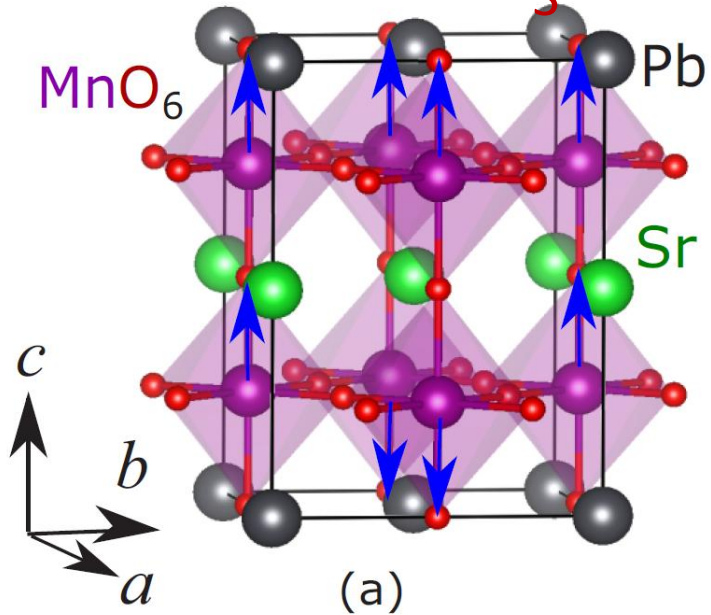
$0.3 \Gamma_5^- + 0.6 M_2^+ + 0.6 M_5^-$



Heterostructure
 PbMnO₃: SrMnO₃
 A robust **POLAR HM FM**

$0.5 \Gamma_5^- + 0.4 M_2^+ + 0.7 M_5^-$
 For PbMnO₃:BaMnO₃

Heterostructure: PbMnO_3 : SrMnO_3



Summary <Polar Half-Metal>

- PbMnO_3 : **HM FM** in ***Pnma*** structure (nonpolar R_4^+ , M_3^+ , X_5^+)
- Nonpolar structure robust against epitaxial strain or substitution
- $\text{PbMnO}_3:\text{SrMnO}_3$ An excellent **Polar Ferromagnetic Half-Metal**
Polarity: Hybrid Improper Ferroelectricity (R_4^+ , M_3^+ , $X_5^+ \rightarrow \Gamma_5^-$)
*uncompensated in-plane off-centering of **Pb** and **Sr***

Arpita Paul and Umesh V Waghmare, Phys Rev B 110, 184110 (2024)

Can we integrate

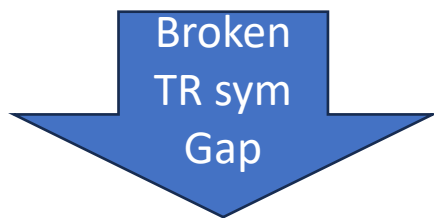
Quantum Geometric Features into Multi-Ferroics? 

Superlattices based on PbMnO_3 and PbVO_3

Strengthen Ferroelectricity through A (6s lone pair of Pb) and B (d^0) sites

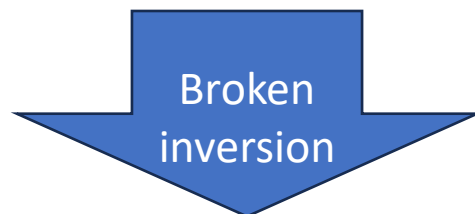
- Mn^{4+} : d^3 versus V^{4+} : d^1
- Mn^{3+} : d^4 versus V^{5+} : d^0

Jahn-Teller, Magnetism



Berry Curvature Dipole
Quantum Geometry

Ferroelectricity



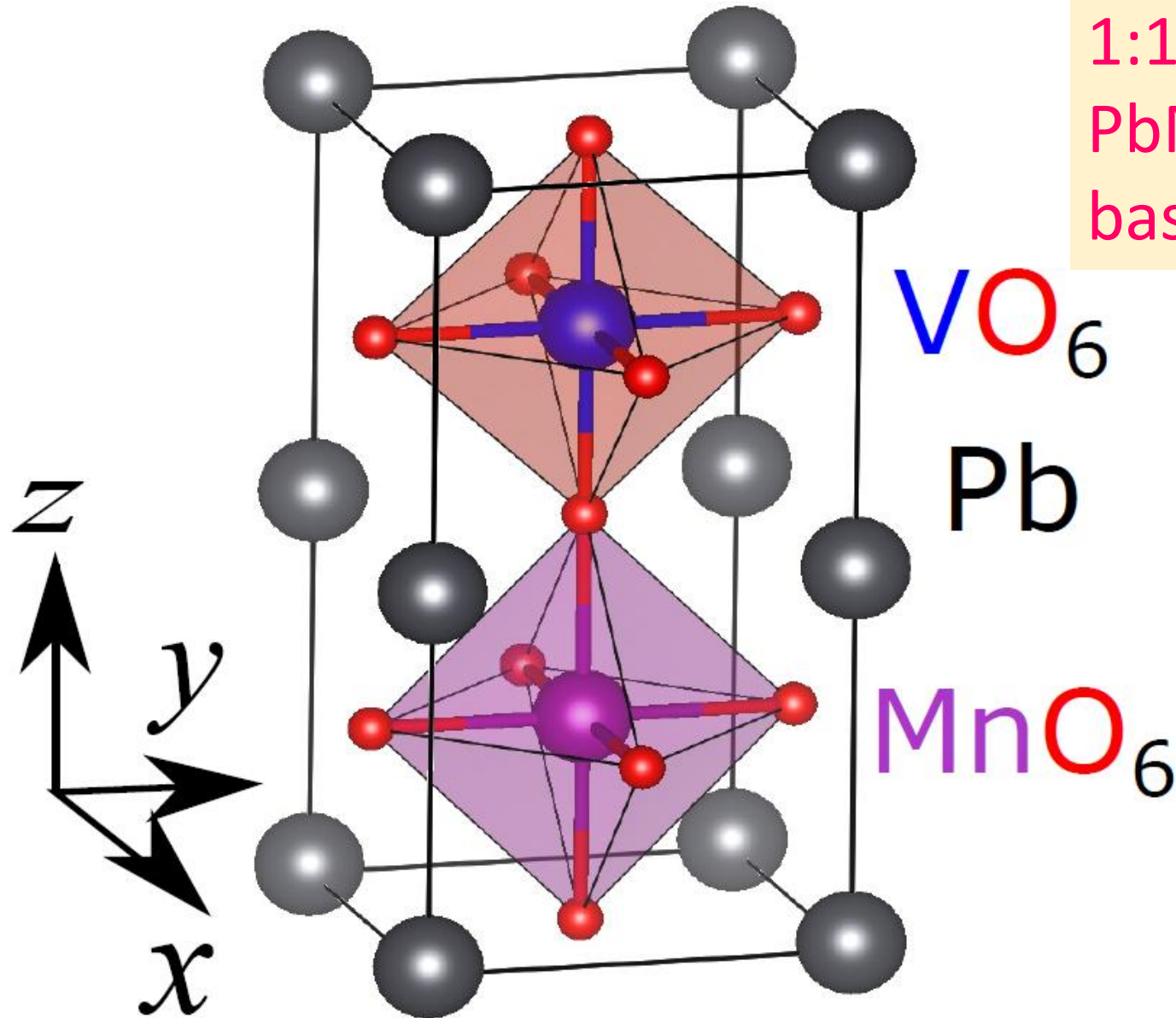
Electric Polarization
Polarity

Possibility of a Tri-ferroic

Magnetization
Polarization
Berry Curvature Dipole

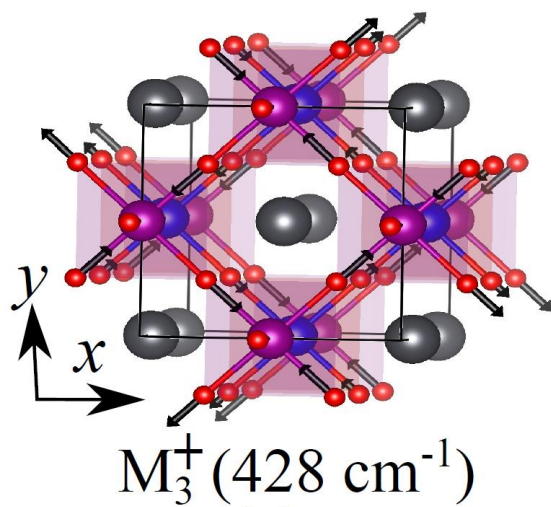
P4/mmm

High Symmetry Structure of
1:1 Superlattice of
 PbMnO_3 and PbVO_3
based on (001) Orientation

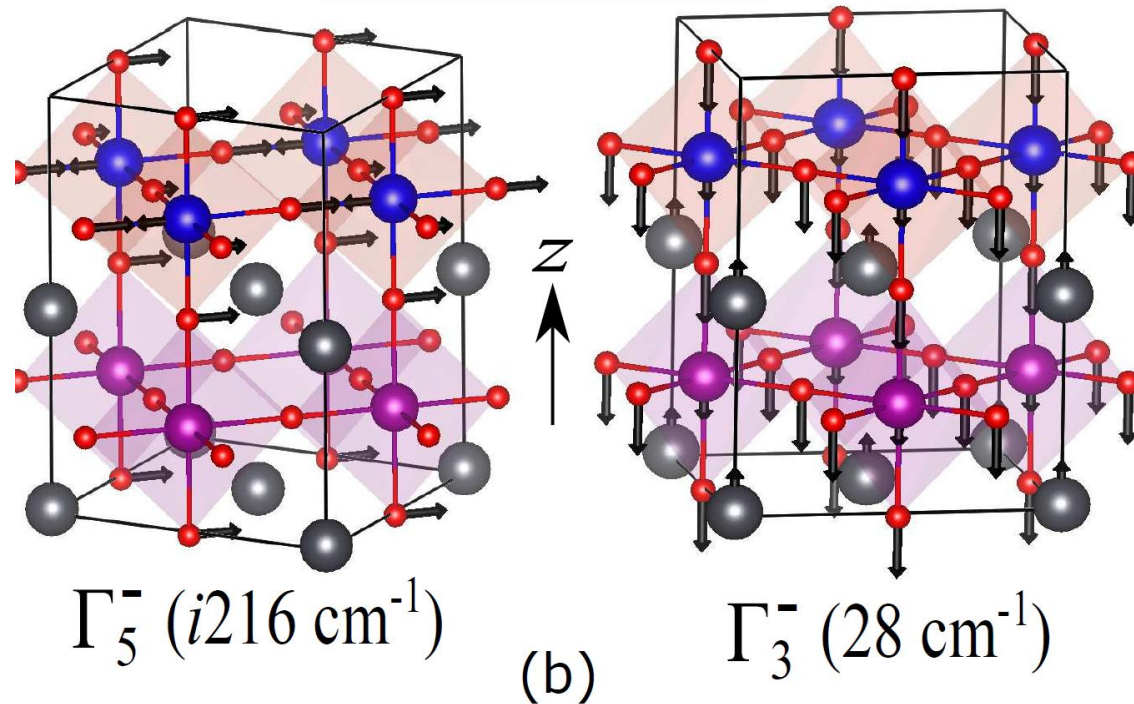


Structural Instabilities of the High Symmetry Structure of 1:1 Superlattice of PbMnO_3 and PbVO_3

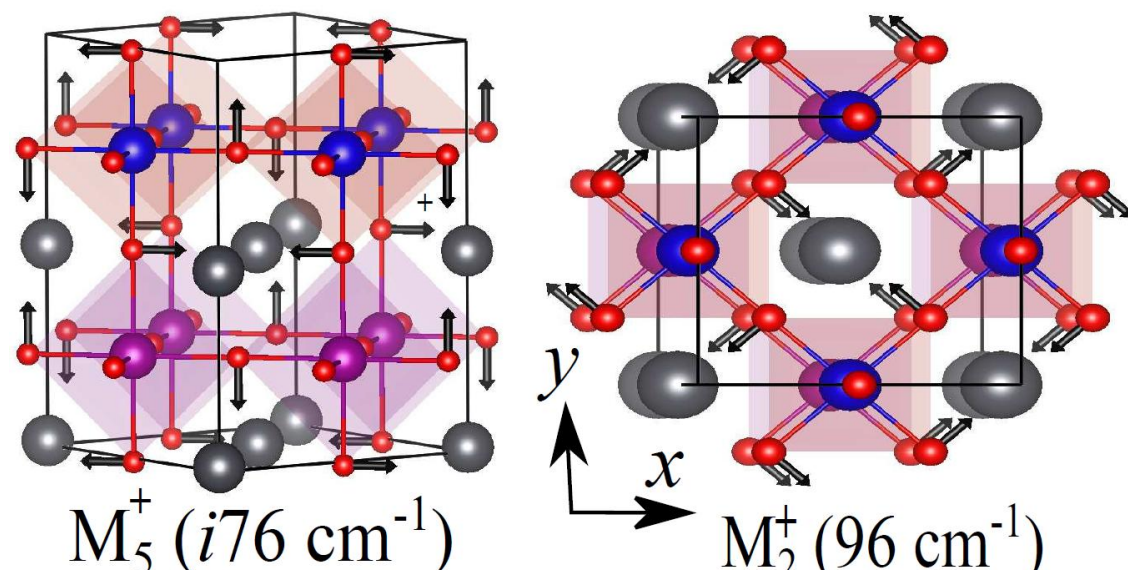
JT distortion



Polar modes



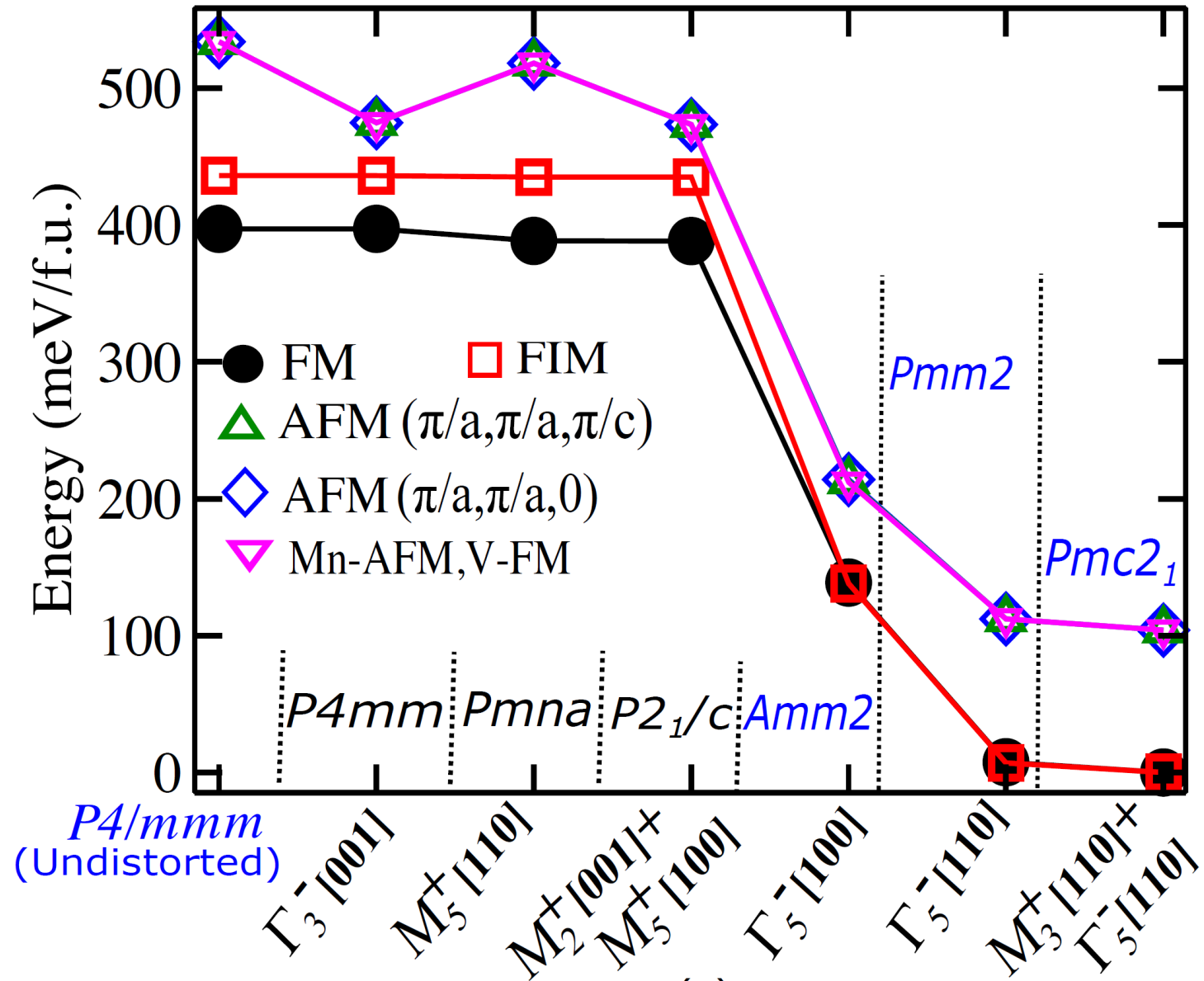
Antiferrodistortive modes



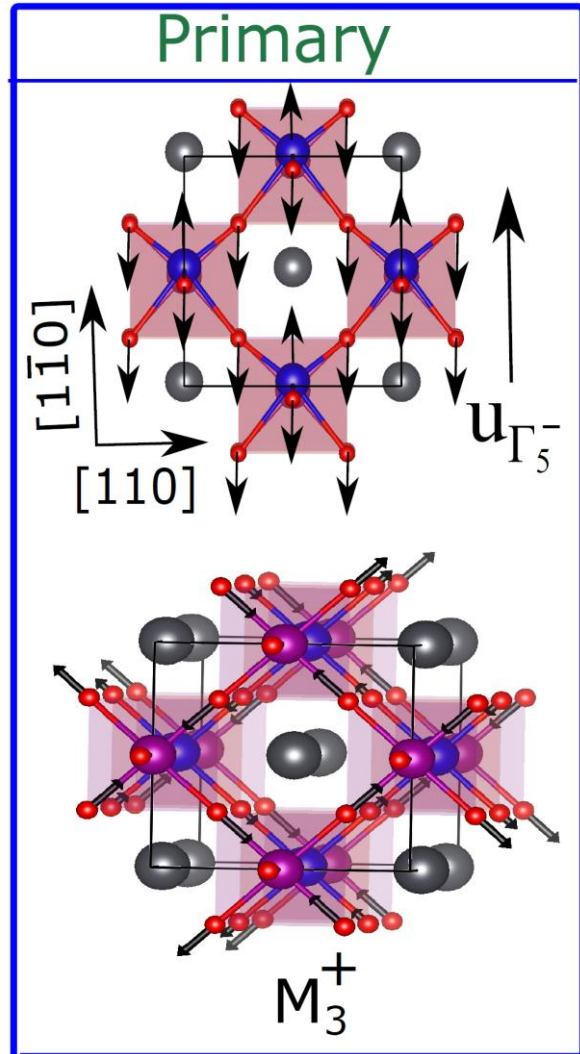
Low Symmetry & Low Energy Structures of

1:1 Superlattice of PbMnO₃ and PbVO₃

- Pmc2₁
Structure is
- Polar
 - Lowest Energy



Order Parameters of $P4/mmm$ to $Pmc2_1$ Structural Transition Superlattice of $PbMnO_3$ and $PbVO_3$



In-plane
Polarization

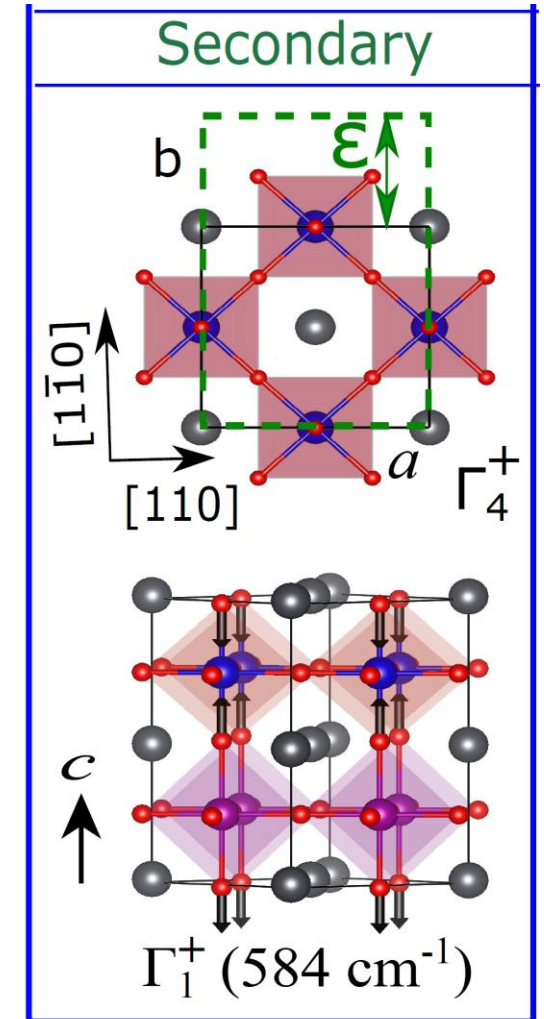
Piezoelectric

b/a ratio
Strain

Jahn-Teller
Distortion:
GAP

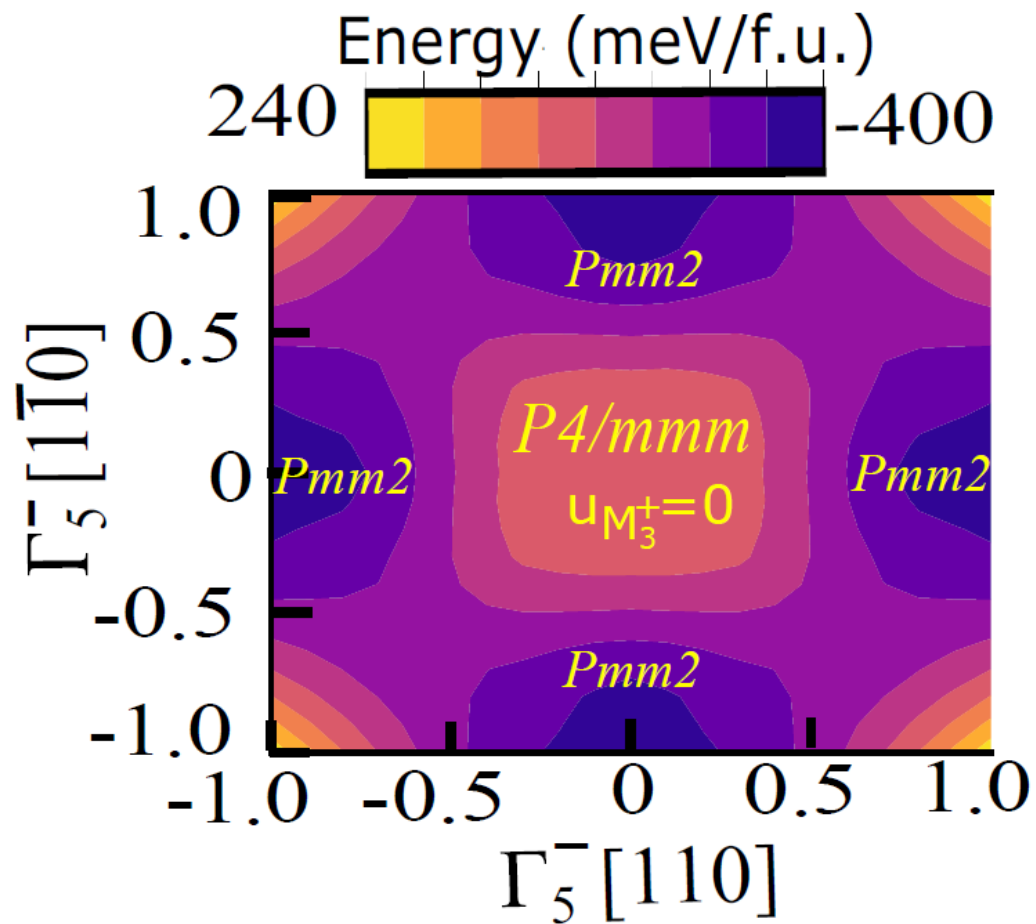
Quantum Geometry

Internal Strain:
Compress VO_6
Stretch MnO_6

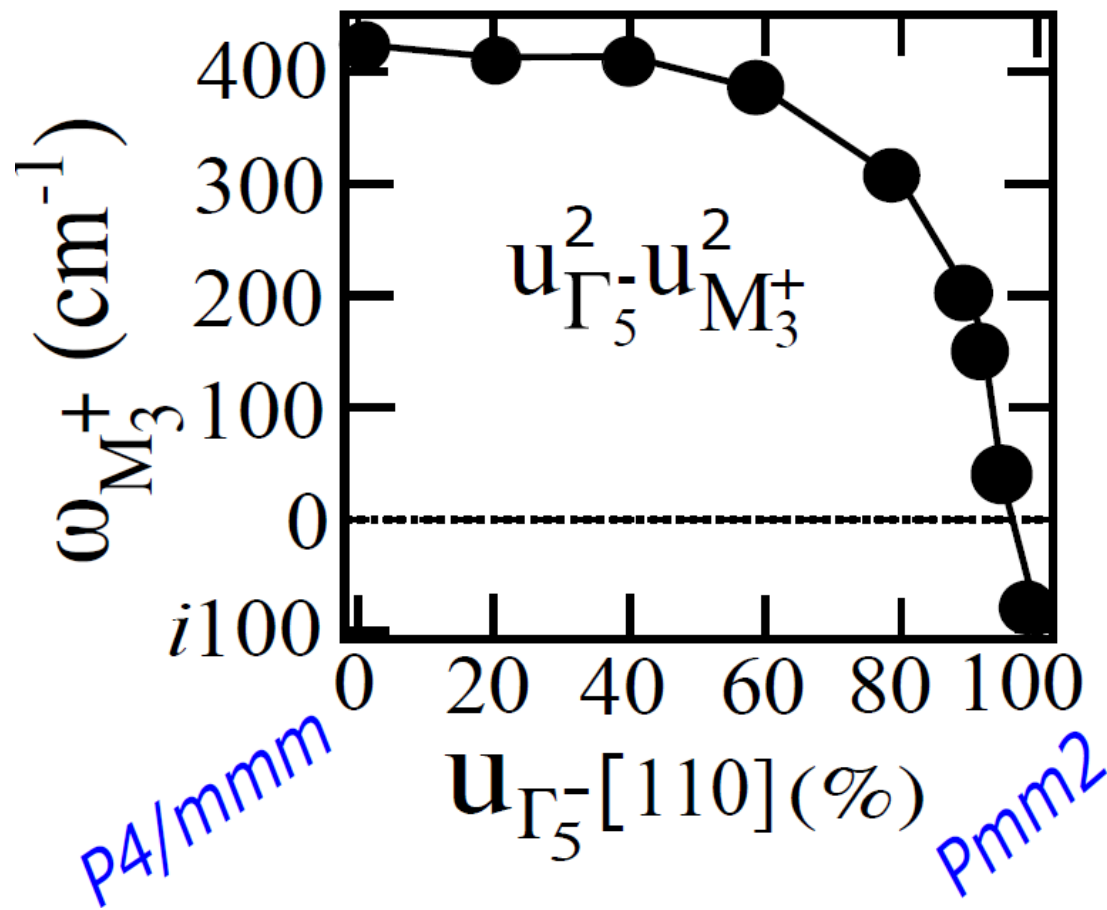


Energy Landscape:

Polar distortion of P4/mmm to Pmm2

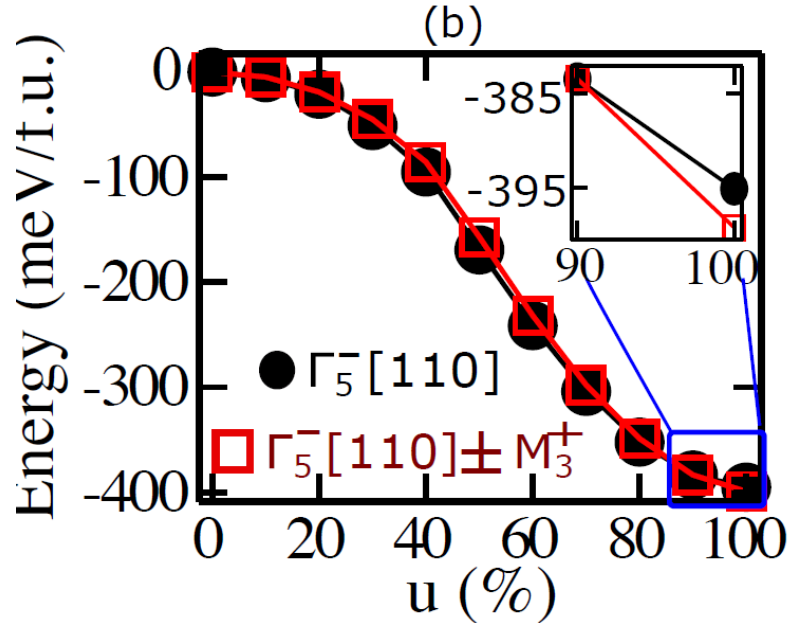


Jahn-Teller Instability

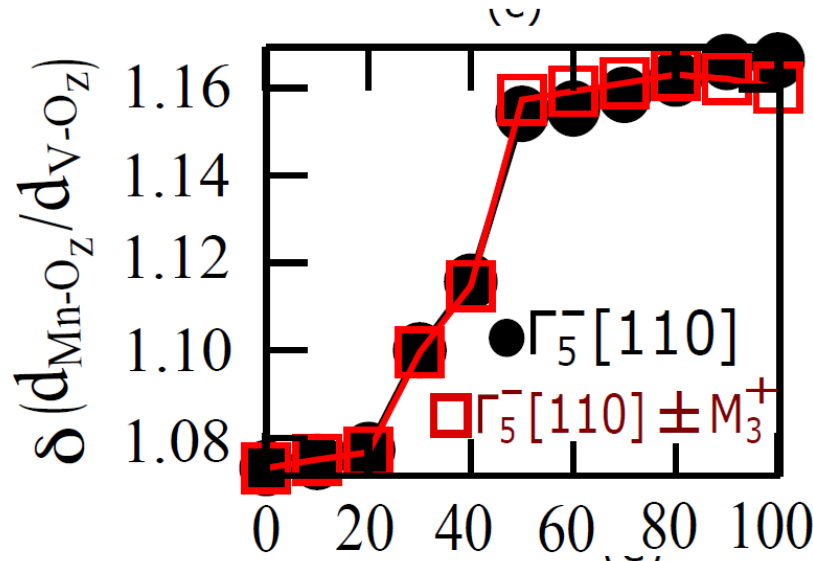
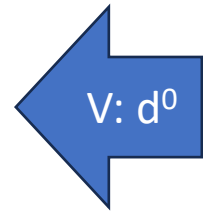


Weak coupling between P [V] and JT [Mn]; sharp change \leftrightarrow nonlinear coupling

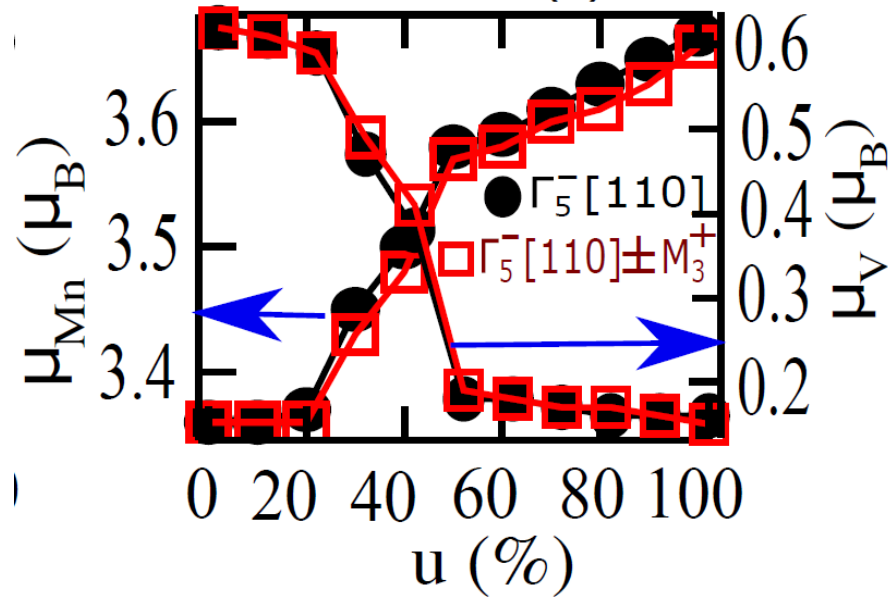
Sharp Changes during $P4/mmm$ to $Pmc2_1$ Structural Transition: Internal Strain and Magnetic Moments



Favor in-plane
polar
distortions



Internal Strain:
Elongation of MnO_6
Compression of VO_6



Magnetic Moments:
e charge transfer
from V to Mn

Electronic Mechanism:

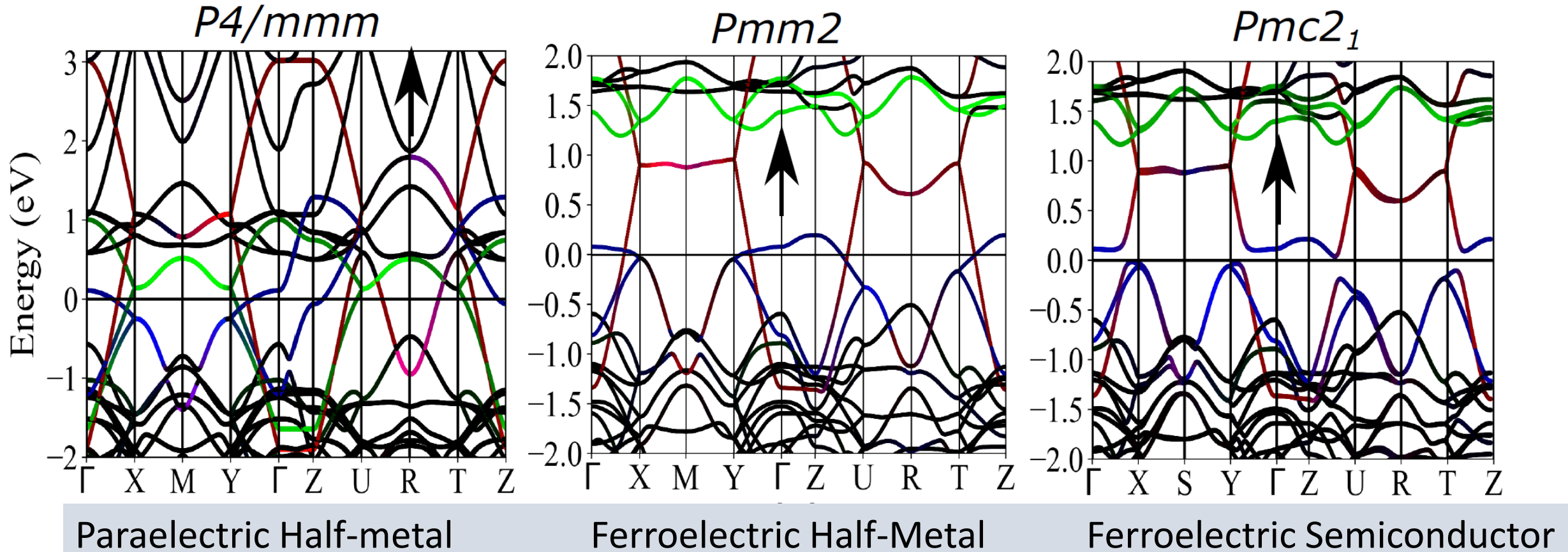
Polar distortion of P4/mmm (**NP**) to Pmm2 (**P**)

| | | | | | | |
|--|------|------|----|----|-----------|-------|
| $\int_{-\infty}^{E_F} \rho_{\text{P}}^{\uparrow}(E) dE - \int_{-\infty}^{E_F} \rho_{\text{NP}}^{\uparrow}(E) dE$ | Atom | xy | yz | xz | x^2-y^2 | z^2 |
| | V | -0.3 | 0 | 0 | 0 | 0 |
| | Mn | 0 | 0 | 0 | 0 | 0.2 |

- e⁻ transfer from V to Mn
- Consequent d⁰ ness of V: polar distortion
- Augmentation of magnetic moment at Mn

- c-compression of PbVO₃ layer: in-plane polar distortion
- Jahn-Teller distortion M₃⁺ mode: *Gap*?

Gap opening: Jahn-Teller distortion



Peierls-like mechanism: Emerging Magnetic Field?

Quantum Geometry

Berry potential:

$$\mathbf{A}(\mathbf{k}) = -\text{Im} \langle u_{\mathbf{k}} | \nabla_{\mathbf{k}} | u_{\mathbf{k}} \rangle$$

Berry phase:

$$\phi = \oint \mathbf{A}(\mathbf{k}) \cdot d\mathbf{k}$$

Berry curvature:

$$\Omega(\mathbf{k}) = \nabla \times \mathbf{A}$$

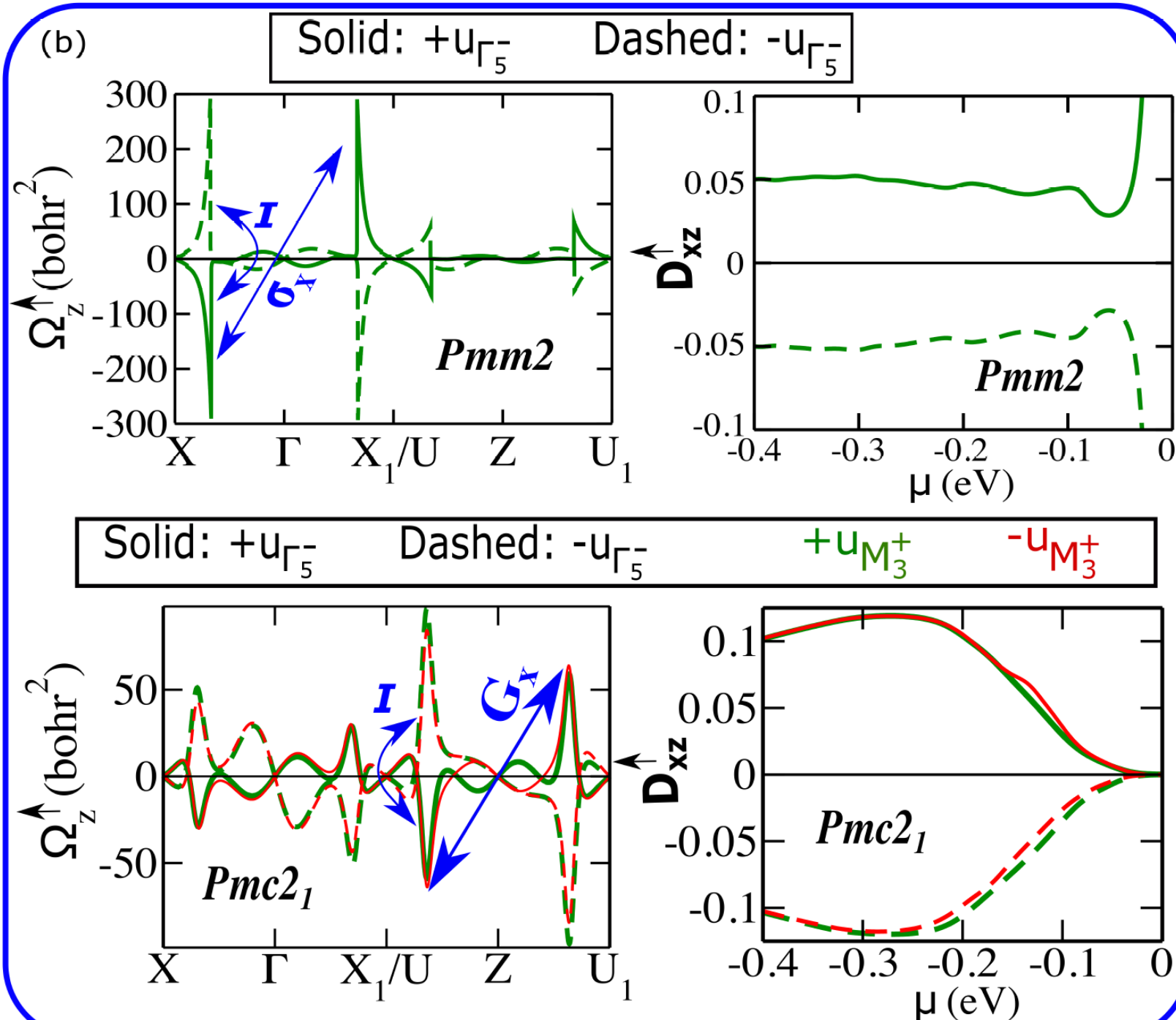
Polarization

Emerging magnetic field

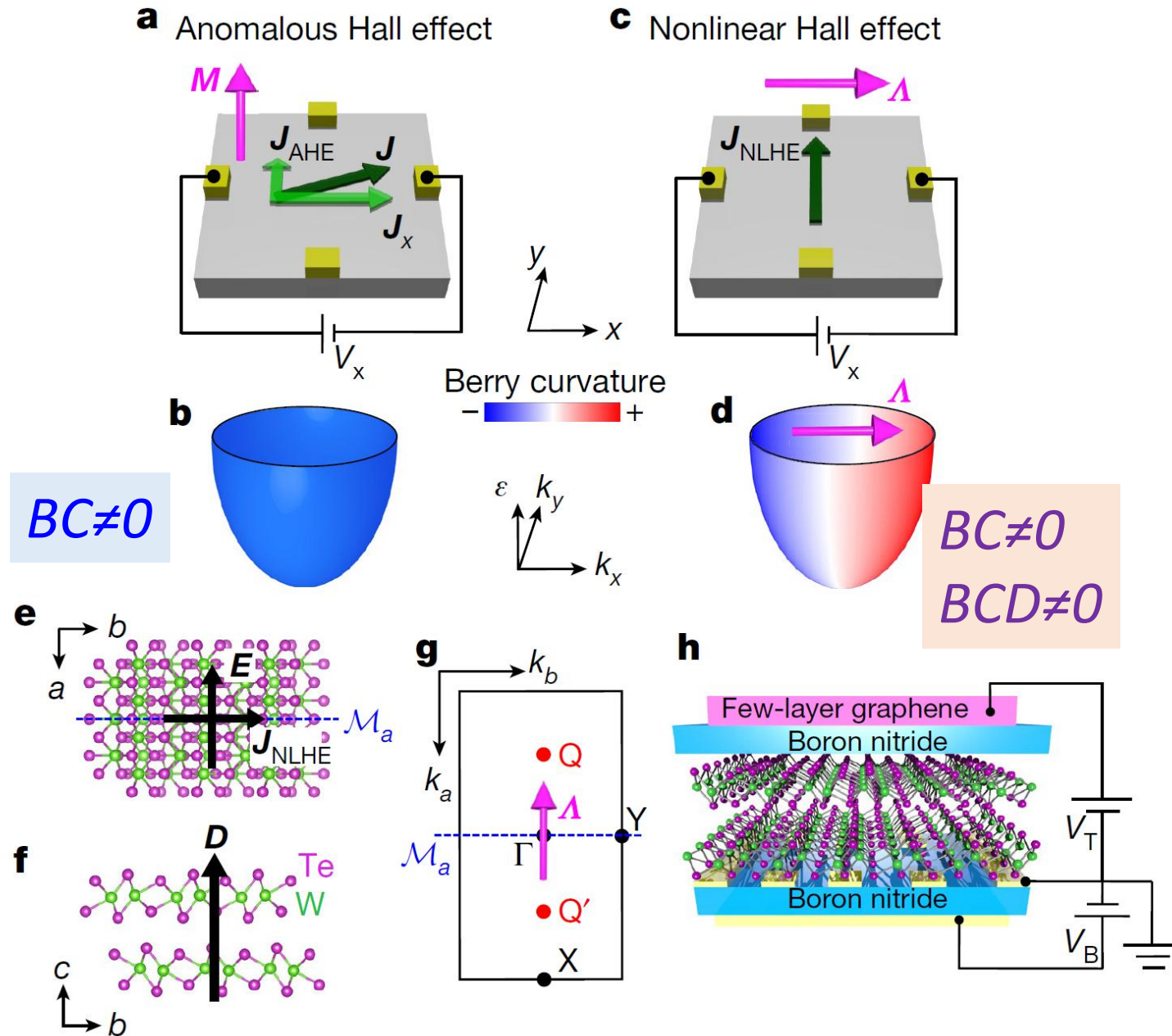
Spin-polarized Switchable

Berry Curvature Dipole:

1. Nonlinear Hall Effect with $B=0$ (anomalous)
2. Coupling with B_{ext} enables E and B control of NLHE



Consequences of Berry Curvature Dipole: *Nonlinear Hall Effect*



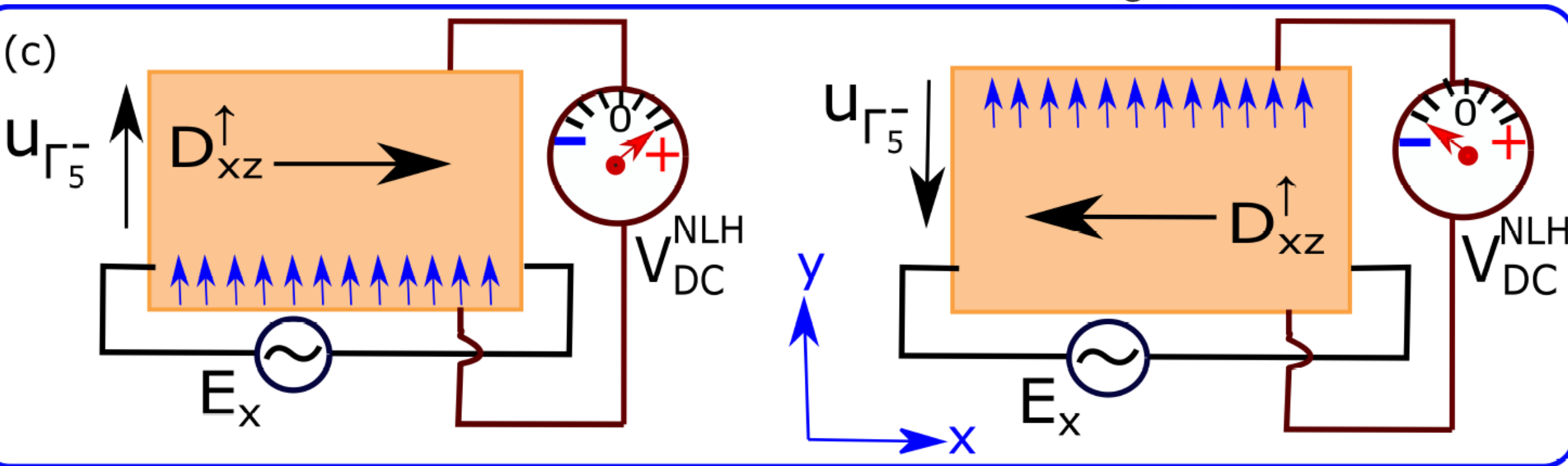
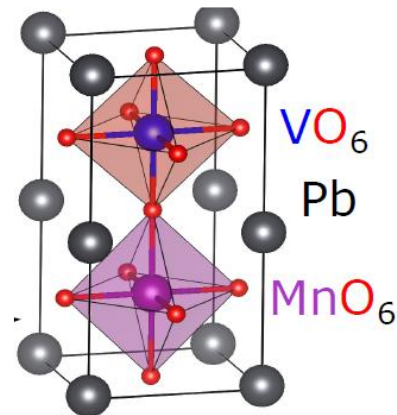
Demonstrated experimentally
in noncentrosymmetric
 T_d -WTe₂ type-II Weyl semimetal
 $\Lambda = BCD \neq 0$

Q Ma et al, Nature 565, 337 (2019)

$B=0$
For driving Frequency ω ,
Hall signals at frequencies
 0 and 2ω

A Multi-ferroic with Switchable

1. Magnetization M
2. Electric Polarization P
3. Spin-polarized Berry Curvature Dipole D



Innovative Device, Exciting Applications Possible!

Nonvolatile Hall Memory

Summary

PbMnO₃:
Half-Metal Ferromagnet
Nonpolar (Pnma)

PbMnO₃: SrMnO₃
Half-Metal Ferromagnet
Polar Half-Metal

Pmc2₁

PbMnO₃: PbVO₃
Magnetic Ferroelectric
Switchable BCD

Hybrid Improper Ferroelectricity
Strong $T_M O_6$ rotational instability

Proper FE

Jahn-Teller Instability

Quantum Geometry

Acknowledgements

Dr Arpita Paul (Indian Institute of Technology, Jammu)